R-10-57

Estimation of residence times of coastal basins in the Laxemar-Simpevarp area between 3000 BC and 9000 AD

Anders Engqvist, A&I Engqvist Konsult HB

September 2010

Svensk Kärnbränslehantering AB
Swedish Nuclear Fuel
and Waste Management Co

Box 250, SE-101 24 Stockholm
Phone +46 8 459 84 00

ISSN 1402-3091
SKB R-10-57

Estimation of residence times of coastal basins in the Laxemar-Simpevarp area between 3000 BC and 9000 AD

Anders Engqvist, A&I Engqvist Konsult HB

September 2010

Summary

The assignment has consisted of computation of the morpho- and bathymetry of the coastal area of Laxemar-Simpevarp for the time period 3000 BC through 9000 AD, in order to estimate the residence times as yearly means of volume-averaged specific age (Average Age, *AvA*) for water in coastal basins. These basins have been selected as belonging to earlier defined biosphere objects, containing anticipated exit points from possible radionuclides leaking from a hypothetical underground repository for spent nuclear fuel.

This endeavor starts with partitioning of the coast into appropriate sub-basins interconnected by straits in an as objective manner as possible. This has been performed in cooperation with Umeå University followed by the transformation of these hypsographical data to a form that can serve as input data to the employed numerical **CouBa**-model. This model has been developed to simulate the water exchange of straits between densimetrically stably stratified basins with a free sea level including advection and mixing of water-borne conservative scalar properties, e.g. salinity, heat and specific age. The forcing of the model consists of run-off, wind-induced stress, thermal surface dynamics (heating/cooling) and density fluctuations at the open boundary toward the coastal zone, relative by which the specific water age is calculated

For these ambient forcing factors there do not exist sufficiently precise climate data other than for contemporary times. For all other time periods the measured and/or model-computed forcing data regarding 2004 have been used. Estimated *AvA*-values for the different time periods are thus an expression of sub-basin configuration and hypsographical differences. An overriding directive has been to rather overestimate than underestimate the residence times, as to avoid underestimation of the subsequent dose calculations.

The results of these *AvA* computations, presented as volume averages of yearly means of the sixteen biosphere object's coastal sub-basins, show not only the anticipated increase of the residence time at the rate of the land rise, but also temporary recessions caused by the transition of different sub-basins being connected or disconnected to the coastal zone. Also an increased amount of run-off water – whose *AvA*-values in analogy to the water of the coastal zone are set to zero – combined with a shrinking volume of the sub-basins as a consequence of the land rise, may be expressed in a such retrograde development.

The unique possibility to check the present results with the *AvA*-estimates of another study occurs for contemporary times, i.e. 2000 AD, and indicates that an undesired underestimation bias may have been achieved amounting to 40% relative to a former study. On top of this level of uncertainty must be added also the contribution of the uncertain climate variations. A first but safely conservative appreciation of the overall uncertainty would depart from a worst-case scenario, namely that the climate variations are in parity with the seasonal variations during 2000 AD. This yields an uncertainty factor 3 for a possible 1 S.D. overestimation of the water exchange rate.

Sammanfattning

Uppdraget har bestått av att utgående från beräkningar av kustens morfo- och batymetriska utformning i Laxemar-Simpevarpsområdet under tidsperioden 3000 BC – 9000 AD uppskatta uppehållstiden i form av årsmedelvärden för volymsmedelvärdesbildad genomsnittlig specifik ålder (Average Age, *AvA*) för vatten i kustanslutna bassänger. Dessa bassänger har tidigare utvalts som de sexton biosfärobjekt som innehåller anticiperade utsläppspunkter från möjligt läckage av radionuklider från ett hypotetiskt underjordiskt slutförvar för använt kärnbränsle.

Detta arbete har primärt inneburit uppdelning av kusten i lämpliga sundavdelade delbassänger på ett så objektivt sätt som möjligt, vilket skett i samarbete med Umeå Universitet, samt att överföra dessa hypsografiska data till en form som möjliggör körning med den numeriska **CouBa**-modellen, som utvecklats för att simulera vattenutbytet mellan täthetsmässigt stabilt stratifierade bassänger med fri vattenyta. Detta inkluderar advekterade och omblandande vattenburna konservativa skalära egenskaper (t ex salinitet, värme och specifik ålder) mellan diskreta bassänger drivet av avrinning, vindstress, termisk ytuppvärmning/avkylning samt täthetsfluktuationer i randen mot den öppna kustzonen, relativt vars vatten den specifika åldern beräknas.

För dessa omvärldsfaktorer har i brist på tillräckligt precisa klimatdata (annat än för nuvarande tid) genomgående uppmätt och/eller validerad modellberäknad drivning för 2004 utnyttjats. Uppskattade *AvA*-värden för de olika tidsperioderna är därför främst uttryck för den skiljakliga hypsografiska utformningen. Ett överordnat direktiv har varit att hellre åstadkomma en överskattning av uppehållstiderna än motsatsen, vilket senare alternativ annars skulle riskera underskattning av efterföljande dosberäkningar.

Resultatet för *AvA*-beräkningarna, presenterade som volyms- och årsmedelvärden för de sexton biosfärobjektens kustanslutna delbassänger, visar inte bara en förväntad stegring av uppehållstiden i takt med landhöjningen, utan även temporära återgångar, vilket beror på att olika delbassänger inom ett biosfärobjekt successivt övertar vattenutbytet med kustzonen. En utökad mängd avrinningsvatten – vars *AvA*-värde i likhet med den för kustzonen satts till noll – i kombination med en med landhöjning krympande bassängvolym kan även uttrycka sig i en sådan retrograd utveckling.

Den enda möjligheten att jämföra de framtagna *AvA*-resultaten uppstår för aktuell tid (det vill säga 2000 AD) och visar en oönskad underskattning uppgående till ca. 40% relativt en tidigare studie. Till denna osäkerhetsnivå måste även osäkerheten avseende klimatvariationer adderas. En första men säkerligen konservativ osäkerhetsuppskattning utgående från ett värsta fall innebärande att klimatvariationerna vore i paritet med säsongsvariationerna för 2000 AD, ger en osäkerhetsfaktor 3 för en möjlig överskattning av vattenutbytet motsvarande 1 standardavvikelse.

Contents

1 Introduction – the assignment

From SKB was assigned 2010-04-07 the task of estimating the water turnover expressed as Average Age (*AvA*) of the coastal zone of Laxemar-Simpevarp area for a time period spanning 3000 BC to 9000 AD with 1,000 years time difference in analogy to a study conducted by DHI /Karlsson et al. 2010/ concerning the Forsmark coastal zone for approximately the same time period but starting from 6500 BC. The present study originally entailed analysis of twelve whole-year cycles but was extended to also include the year 2000 BC. The objective was originally focused on 17 topographically defined so-called *biosphere objects* (BOs) that have in common inferred exit points reaching the surface land and water ecosystems via the geosphere surrounding the hypothetical location of a nuclear repository. The delimitation of these BOs is shown in Figure 1-1a with the shoreline of the contemporary time period (2000 AD) as the reference background. The associated exit points are displayed in Figure 1-1b. Two of these BOs were subsequently conjoined into one area. These basins go through a succession of being a part of the open *coastal zone* (CZ) to be gradually more landlocked and finally in some cases become lakes detached from two-way exchange with the coastal zone. Finally they become part of the land ecosystem. For the time period they are connected to the CZ, they are subjected to sedimentation processes. This work is thus based mainly on the consequences of land rise and subsequent water levels and may be subdivided into four phases:

1. First should be determined for each of 13 whole-year cycles between 3000 BC and 9000 AD if a configuration of hydraulically interfaced basins and straits exists in the form of embayments that connect to the costal zone and for which any of 17 identified BOs is a part.
2. The bathymetrical data should be determined for all basins and straits of the actual configuration from the innermost basins to the straits that connect to the open coastal zone. This subtask entails detailed specification to be carried out at Umeå University. Also the size of the corresponding catchment areas for the respective basin must be analogously determined in order to estimate the freshwater discharge. The water exchange is to be computed in the form of *AvA*-values with regard to the different BOs and is accounted for with regard to the different biosphere objects. The wet areas of any particular BO thus must be partitioned in two or more *sub-basins* (SBs) and that additional such SBs outside the BOs may be needed to arrange for an acceptable partitioning of the coast from a physical oceanographic point of view. The SBs will thus be the basis of the computations and the BOs for the accounting of the results.
3. With the forcing (boundary variation of salinity, temperature and sea level in combination with wind-induced mixing and forced surface water temperature) that has been established for 2004 in an earlier model of the same area /Engqvist and Andrejev 2008/ the 13 one-year long cycles are modeled using the **CouBa**-model that resolves the different areas into hydraulically coupled discrete basins. In order to obtain initial values, the model is spun-up one full year for each of the 13 analyzed time periods and the oceanographic state by the end of such year-cycle is iterated to serve as initialization state for the actual runs. Ice conditions are supposed to be analogous to the model forcing year 2004, which also must be presupposed to apply to the other twelve time periods.
4. The collective *AvA*-values that are finally computed will be expressed as fraction of a year and represent the age of the water relative the open CZ. A conservative estimate of the *AvA* of the CZ may subsequently be added to the *AvA* of the BOs.

In addition to *AvA*, the introduced abbreviations **BO** for biosphere objects, **SB** for sub-basins and **CZ** for the coastal zone will henceforth be used in this report.

Figure 1-1a. *Subdivision into biosphere object (BO) basins enumerated 201 through 216 against the background of the contemporary coastal shoreline (2000AD) when the sea level is 1m above the yearly mean water level (MW). The minute BO 217 was defined on an early stage of the study but was subsequently conjoined with BO 216.*

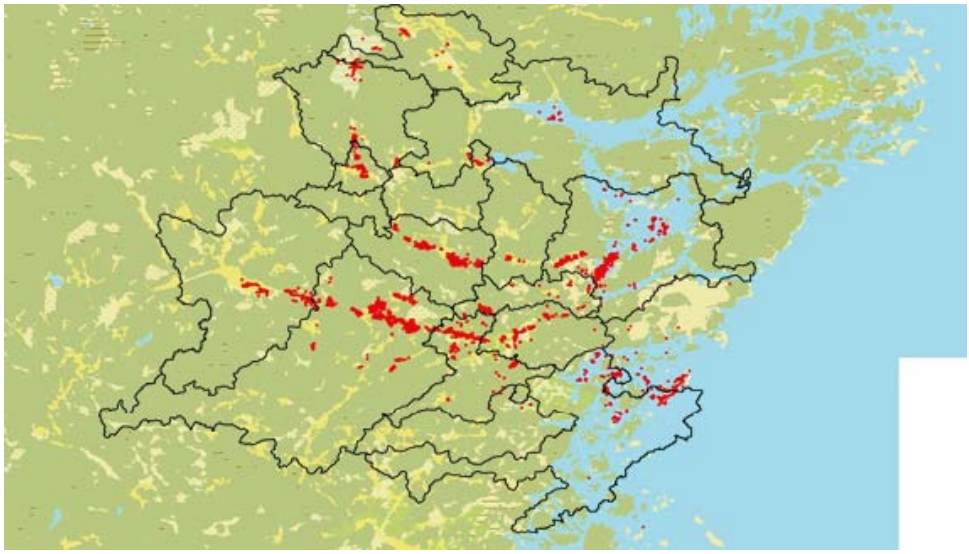

Figure 1-1b. *Location of the anticipated exit points from possible radionuclides leaking via the geosphere.*

2 Coastal oceanography of the Laxemar-Simpevarp region

2.1 Contemporary coastal bathymetry

The bottom along the Laxemar-Simpevarp coast gradually slopes in the offshore direction; there are few topographic features that naturally indicate a well-defined delimitation line, Figure 2-1. The major island Öland to the east acts to a large extent to shield off oceanographic impacts from the east and south. The contemporary (2000 AD) coastal area (Figure 2-2) has been partitioned in an earlier study /Engqvist 2006/ into a number of non-overlapping water areas based on assessment of the present-day bathymetry using GIS methods and complementary sounding of less well-resolved features – mostly straits. This partitioning will subsequently be compared to the present one but at this stage it suffices to note the locations indicated by R-1 through R-4 where the oceanographic forcing of the coastal model (salinity and temperature profiles together with sea level fluctuations) is provided by the 3D-model that computed these data. The subdivision and labelling of the water areas in Figure 2-2 are thus only used to give the concomitant naming and to serve as a counterpart of the comparison which will be performed in the discussion Chapter to follow.

The BOs of the present study coincide with anticipated exit points connecting to the geosphere. These BOs combined with computed bathymetrical data of the different time instances have served as the basis from which the present set of SBs are inferred. The water exchange of such a particular SB area relative to the Baltic Sea can be achieved in two steps. First, all of these SBs are collectively subjected to estimation of their *AvA*-measure, counting only the CZ water as exogeneous with its inherent *AvA* set to zero, thus defining the reference area to which the relative water exchange is counted. Also freshwater run-off is considered as exogeneous. Second, the *AvA* of the CZ relative to the Baltic is computed. The uncertainty of this method with regard to the bathymetry may be estimated by comparing the *AvA*-values that ensue when two different subdivisions and hypsographic data sets are compared.

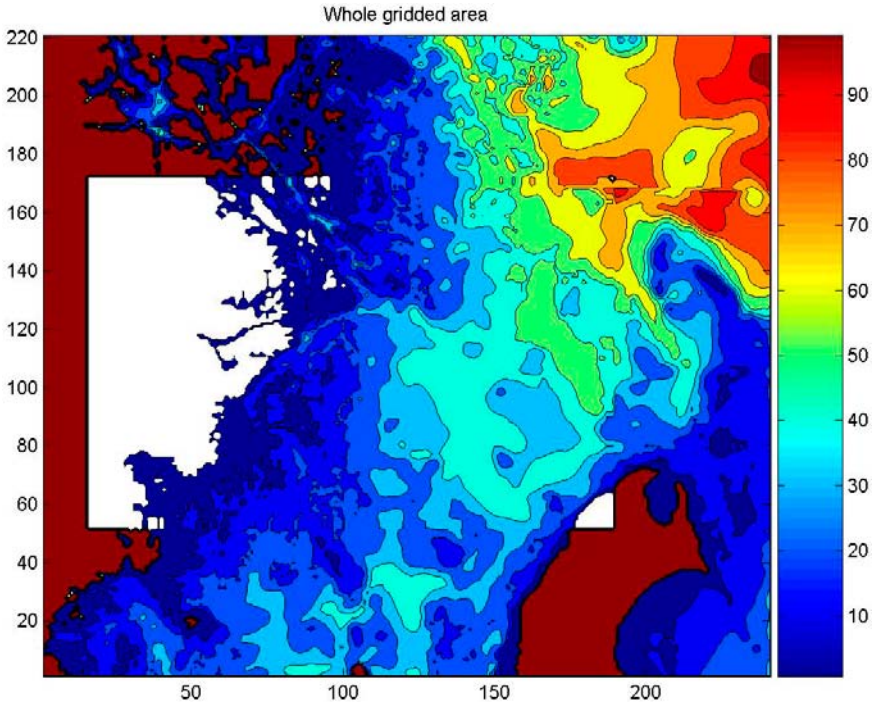

Figure 2-1. *Overview of the contemporary (2004) average water depth (at MW) in [m] showing the entire Laxemar-Simpevarp area that was gridded from digital charts /Engqvist 2006/. The chosen model grid for the AS3D-model computations is indicated with a broken white line.*

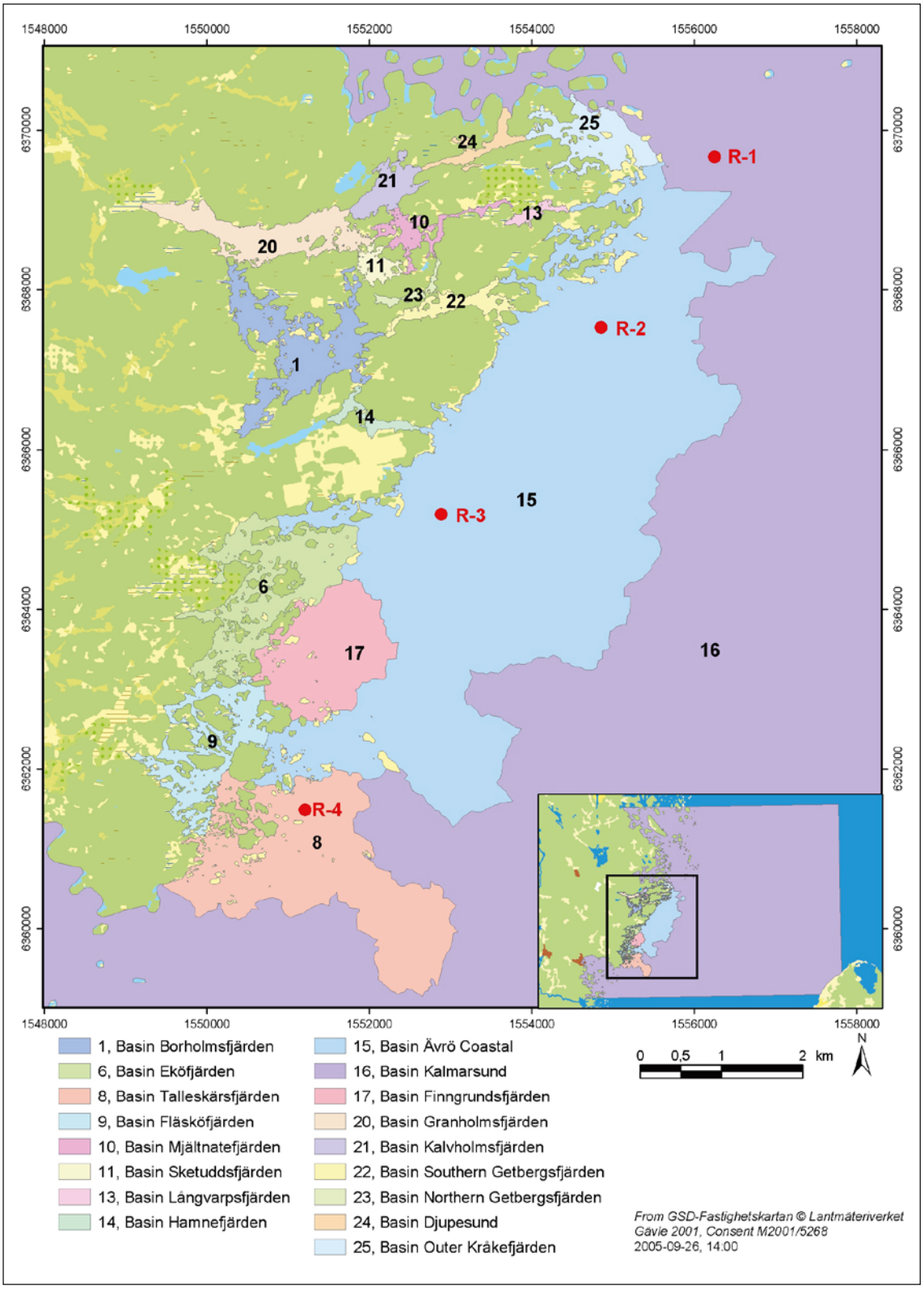

Figure 2-2. *The partitioning of the contemporal Laxemar-Simpevarp coastal zone (CZ) into water areas together with their naming in /Engqvist 2006/. The CZ in this earlier study consisted mainly of the water areas 15 and 16 together with the outer parts of water areas 8 and 17. The locations for which the density profiles computed by a 3D-model are used to force the DB-model have been indicated by R-1 through R-4 (bassangindelning_20050926_1400.mxd).From /Engqvist 2006/.*

2.2 Transition from open coast to lake

The resulting bathymetry of the Laxemar-Simpevarp coast as a result of land rise and long-term sea level change /Brydsten and Strömgren 2005/, complemented with sedimentation dynamics /SKB 2010a/ has been computed by Umeå University. Since the land rise historically has exceeded the sea-level increase, the transition basically characterized by underwater features such as ridges undergoes an evolution to become shorelines as the land progressively rises. The BOs will eventually become lakes with only one-way water exchange relative to the coastal waters. Eventually they will thus belong to land ecosystems in the form of bogs or other forms of wetlands.

2.3 Water exchange transition

The water between coastal basins flows freely above the sill level of the strait that connects them. This exchange is subjected to restrictions that the forcing (*barotropic* concerning sea level differences and *baroclinic* concerning the density differences with regard to depth) defines: the dominant mechanisms of these have been incorporated into the employed **CouBa**-model /Engqvist and Stenström 2004/ which has been thoroughly validated /Engqvist and Stenström 2009/. In addition to these features it has been considered as essential to also implement the mechanisms that decide when a basin no longer can exchange water with the coastal zone. For flows with uniform density (the purely barotropic case) it is simple to formulate the criterion. If the Froude number (a *dimensionless number* defined as the ratio of a characteristic velocity to a depth-dependent gravitational wave velocity) somewhere in the pathway that connects the two basins exceeds unity, these basins are hydraulically decoupled from a two-way exchange with one another. For baroclinic flows with varying density the blocking condition is more complicated. A first type of blocked exchange occurs when the most dense bottom layer gets arrested while still present in the strait. Two-way exchange may still occur through the strait by the slow process of diffusion. A more definite blocking occurs when the sea level difference is sufficiently intense to flush this layer off the strait. This can theoretically only happen when the strait possesses a rectangular cross-section. For other geometrical shapes there will always be a thin layer of stagnant dense water present /Dalziel 1992/ in the deepest part of the strait. In the present study this latter criterion of blocking of exchange will be used.

3 Methods

3.1 The CouBa-model

As the naming of this employed model (**CouBa** for **Cou**pled **Ba**sins) implies, it computes the water exchange (including a number of water-borne scalar properties such as *AvA*) of a set of discrete hydraulically coupled basins. This model concept has been developed in stages since the first employment in SKB context /Engqvist 1997/. It has been validated both concerning its capacity to simulate measured salinity and temperature profiles and also to simulate the strait exchange current /Engqvist and Andrejev 2008, Engqvist and Stenström 2009/ with fully acceptable and convincing validating results.

3.2 The Average Age concept

The Average Age (*AvA)* has been used as a measure of the water exchange rate since the mid 1990s /England 1995, Engqvist 1996/. This concept has progressively earned a growing international acceptance /Deleerschnider et al. 2001/. It has been used in numerous SKB publications e.g. /Engqvist et al. 2006/ in which paper a thorough and pedagogical description is given. The use of this measure for water turnover is thus a natural choice in this study and does not seem to need further motivation or description.

3.3 Extraction of basin and strait configuration, hypsography and catchment areas

The hypsographic curves of basins and straits have been extracted by Umeå University from a digital elevation model (DEM) enhanced with sediment alterations. This cooperation necessitated precise hand-shaking conventions to specify the relevant cartographic information. These specifications have been deferred to Appendix A (figure references to this appendix are indicated with a leading 'A') together with the resulting configurations of coupled discrete basins (referred to as SBs) – one for each of the 13 time periods – for which the **CouBa**-model subsequently computed the resulting *AvA*-values. According to Appendix A one or more of these SBs constitute the different BOs. Once the configurations were determined, the actual hypsographic data of the basins could be extracted in a form suitable for model purposes in a straightforward manner. The specification procedure in communication with Umeå University can be listed in the following twelve points.

1. If the locations of water areas one meter above mean water level (MW) are in the form of a simple conjoined area (see e.g. BO 214 on the map for 3000 BC, Figure A-1a), such areas are denoted with the corresponding BO number ranging from 201 through 216. For the model computations the SBs and straits in the configuration diagrams are relabeled in consecutive order with a leading B and S respectively.
2. If the appropriate partitioning of two adjacent basins from a coastal oceanographic point of view coincides with the delimitation between these basins (e.g. as for 205 and 207, Figure A-2b), this strait is denoted 205/207 and is drawn in the configuration diagrams as black solid lines. Such borders automatically coincide with thresholds.
3. If the water areas within a basin occur in several non-connected coastal basins or if there are coastal oceanographic motives to make a finer subdivision of a conjoined area, then these SBs are marked with an order number trailing the BO number after a hyphen-sign. Such interfaces are marked both in maps and configuration diagrams with dashed bold lines.
4. The peripheral SBs that specifically are motivated to be pointed out as belonging to the CZ are indicated with a trailing zero. A SB of the numbered basin that due to a sufficiently large section area of the strait interface is considered as belonging to the coastal zone is consequently denoted with a trailing zero after the basin number, e.g. 205-0.

5. Complicated and very wide interfaces between two basins (e.g. 202 and 203 for 3000 BC, Figure A-1a) may be a motive to conjoin them which is indicated with a double directed arrow in the *maps*.
6. A single-headed arrow in the *configuration diagrams* indicates a strait with a threshold above the MW level and the arrow is in the direction to which the freshwater will flow when the sea level is below the sill crest. A double-headed arrow in the same diagrams indicates that it cannot be inferred from the configuration diagram alone in which direction the fresh water will flow when the sea level of the coastal zone is low. It can certainly only flow one way at a time.
7. For physical oceanographic reasons there are strong motives to include auxiliary SBs that are outside the BO areas. Their inclusion acts to increase the residence times. Such new coastal SBs are denoted 'New1', 'New2' and so on until all needed auxiliary SBs are accounted for.
8. In the rectangle in the configuration diagrams representing the CZ it is indicated which sub-basin if belonging to a BO (or a SB thereof) is on the CZ side of a strait.
9. Parallel straits may either be explicitly drawn or can be tacitly conjoined into one resulting strait.
10. The road banks that occur from 2000 AD and onward in time may be concealed under basin interfaces. These have been accounted for in the data extraction process.
11. SBs that are far off the anticipated nuclear exit points have not been considered as relevant to include, e.g. the mid section of BO 216 (Figure A-1a).
12. The conversion of data extracted from the DEM to hypsographic information: for basins, the areas with regard to depth are readily summed from the bottom-most area to one meter above the MW level to obtain the hypsographic curve.

The above guidelines resolve most but not all possible complications, so admittedly a certain degree of subjectivity can still arise in the process of partitioning into the configuration of SBs.

For the ensuing straits interconnecting the SBs, the procedure is somewhat more complicated. First the depth along the interface of two adjacent basins is extracted from the DEM. For straits with a decided main direction, their cross-section areas along the deduced delimiting sill ridges, is projected perpendicularly to this main direction. For more complicated arrangements with straits pointing in various directions and with varying widths, these have been treated individually and are accounted for as operating in parallel. In Figure 3-1 are given two examples – one single depth strait and one more complicated – as how the strait hypsographic data are extracted from output of the DEM.

An overview of the number of basins and straits with regard to the thirteen different time periods is given in Table 3-1 and the partitions of the BOs for the same time periods into SBs (according to Appendix A) are presented in Table 3-2.

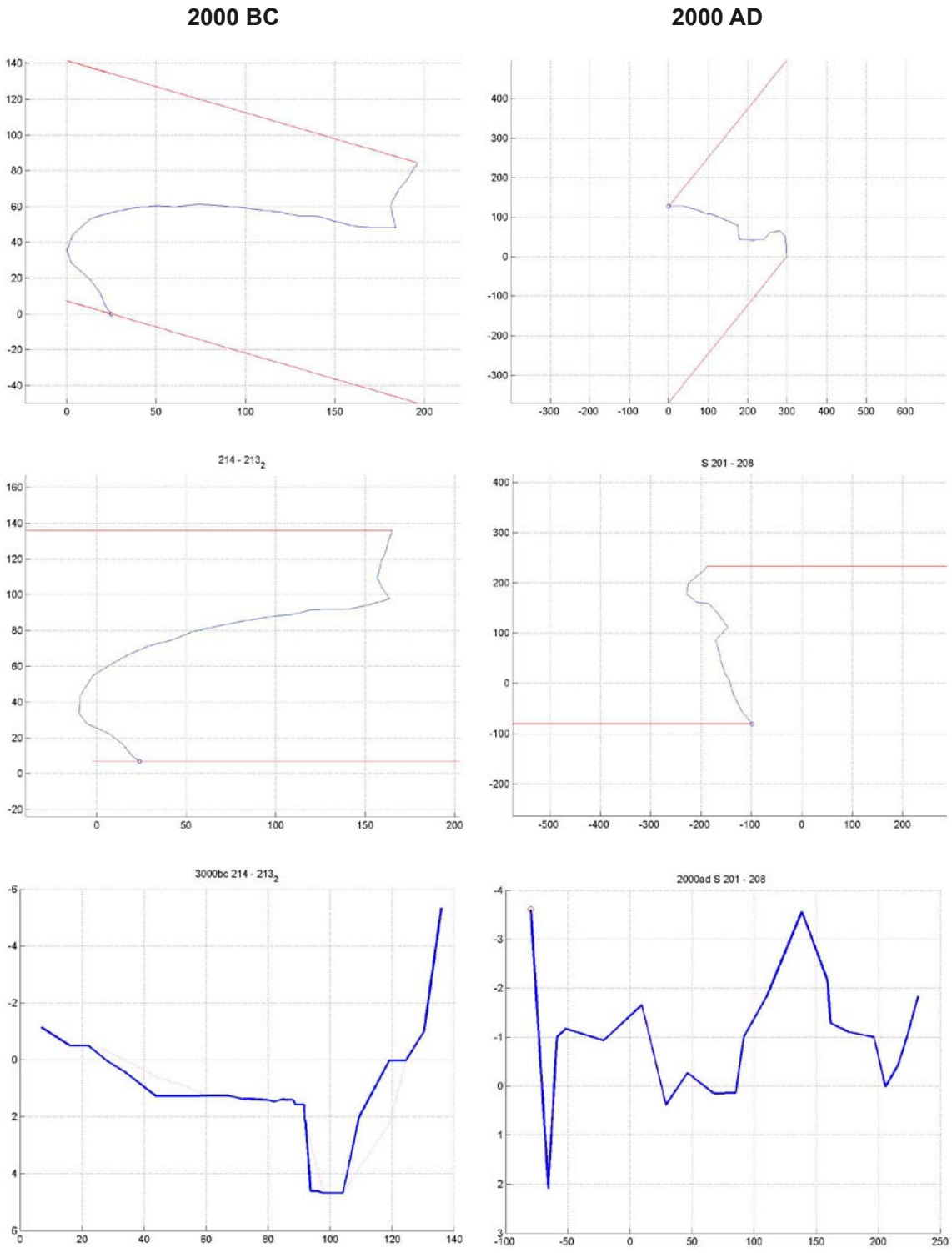

Figure 3-1. *Examples of how the extraction of the strait hypsographic data is performed. This procedure starts with the strait interface plotted in the DEM coordinate system (blue lines in the top diagrams). The second row shows the same interface but with the coordinate system rotated so that the main flow direction is aligned with the x-axis, depicted with red lines. The third row shows the projected cross-sections on the y-axis. The diagrams in the left column are examples from 2000 BC and represent a strait with just one deep section with monotonously sloping sides to either shore; the right column from 2000 AD shows a more complex cross section design. The width for each meter (starting from 1m above MW level is assessed. For the simple straits (left columns) this extraction can be done by algorithmic coding. The red dotted line shows an early but discarded such attempt. For the more complex cross sections graphical extraction has proved to be a faster method with approximately equal accuracy.*

Table 3-1. Overview of the number of basins and straits when partitioning the Laxemar/Simpevarp coast for the different time periods according to the specified guidelines in Chapter 3.3.

Number of features	Time periods 3000 BC	2000BC	1000 BC	0 BC/AD	1000 AD	2000 AD	3000 AD	4000 AD	5000 AD	6000 AD	7000 AD	8000 AD	9000 AD	Total
Accounted basins (BOs)	4	8	4	6	5	6	3	2	1	1	1	1	1	43
Modeled basins (SBs)	9	11	9	10	8	15	12	8	8	4	1	5	5	105
Modeled straits	10	15	9	10	12	22	13	10	9	4	1	7	6	128

Table 3-2. Overview of how the BOs are partitioned into SBs. The numbers refer to the schematic rendering of the configurations in Appendix A. Contrary to Table 3-1 which lists all SBs needed for the computations, this table only entails only the SBs that are contained within the BOs affected by exit spots.

Time period	Biosphere Object (BO)	Sub-Basin (SB)
3000 BC	202 and 203	3
	214	6
	213	7, 8, 9
2000 BC	203	3
	202	4
	201	5
	205	6
	207	7
	213	8, 9
	212	10
	217	11
1000 BC	201	1, 3
	207	2
	212	4
	211	5
0 BC/AC	201	1, 2, 3, 5
	207	4
	209	6
	212	7
	211	8
	216	9
	215	10
1000 AD	201	1
	208	3
	211	4
	216	7
	215	8
2000 AD	201	1
	209	6
	208	7
	211	9
	216	14
	215	15
3000 AD	201	1, 4
	208	6, 8
	215	12
4000 AD	201	4
	215	8
5000 AD	215	8
6000 AD	215	1, 2
7000 AD	215	1
8000 AD	215	1, 2
9000 AD	215	1, 2

4 Model input data

In absence of sufficient knowledge and detailed understanding of the climate variation and its subsequent expression in terms of the physical forcing of the **CouBa**-model (for all 13 one-year simulations equally spaced in the time-bracket 3000 BC through 9000 AD) has been adopted from the data set pertaining to 2004 /Engqvist and Andrejev 2008/. This in analogy to the procedure followed by /Karlsson et al. 2010/. These data include salinity and temperature stratification profiles along the Laxemar-Simpevarp CZ together with sea level fluctuation and have been validated against measurement data /Engqvist and Andrejev 2008/. During 2004 there was a comparatively mild winter with virtually no ice formation in the coastal waters. Initialization data has been obtained by spinning up the model by running the model with identical forcing (of the year 2004) for one full year prior to the actual run.

4.1 Meteorological forcing

The wind forcing is from the closest SMHI weather station located at Ölands Norra Udde, Figure 4-1. These local data correlate well (ρ = 0.84) with the Mesan-dataset used for computing the boundary forcing /Engqvist and Andrejev 2008/. The precipitation will be accounted for below when treating the freshwater discharge.

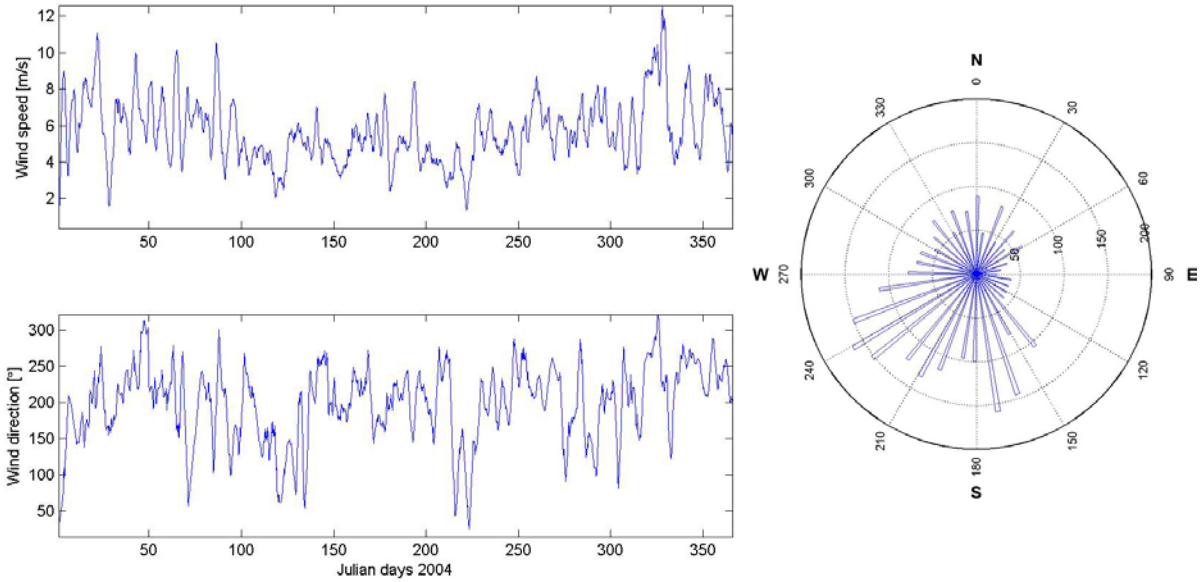

Figure 4-1. *Wind forcing measured at Ölands Norra Udde during 2004. The top diagram shows the wind speed filtered with a 6-day running average; the lower left similarly filtered wind direction. The windrose (right) shows that the prevailing wind direction is from the SW.*

4.2 Boundary forcing

The boundary forcing consists of sea level (Figure 4-2), salinity (Figure 4-3) and temperature (Figure 4-4). These data have been excerpted from the computation of the corresponding fields (station R-1 in Figure 2-2) employing the AS3D-model /Engqvist and Andrejev 2008/ and have been demonstrated to correlate acceptably well with measured data for 2004 which unfortunately could not be assessed for the entire calendar year.

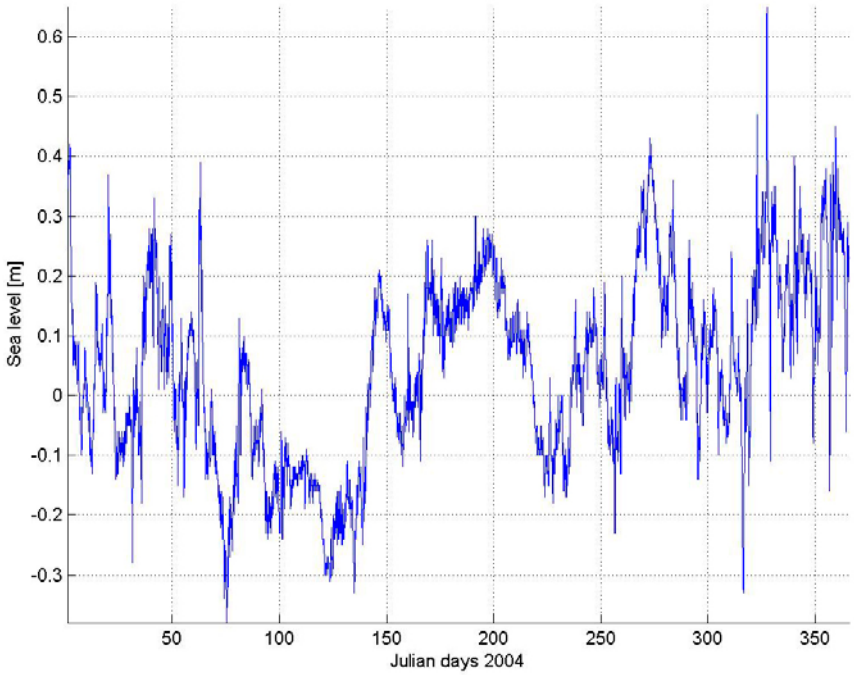

Figure 4-2. *Sea level fluctuations outside the Laxemar/Simpevarp coast (Station R-1) as computed by the AS3D-model /Engqvist and Andrejev 2008/. The peak occurs in late November (approximately Day 320) and amounts to +68 cm.*

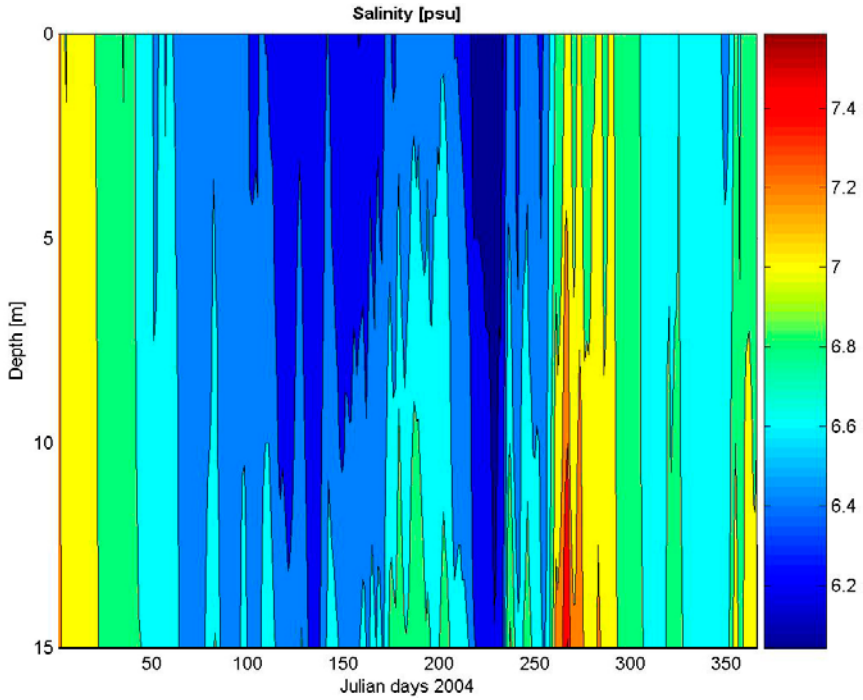

Figure 4-3. *Contours of salinity variations (psu) at the station R-1 (Figure 2-2) as computed by the AS3D model /Engqvist and Andrejev 2008/ for 2004.*

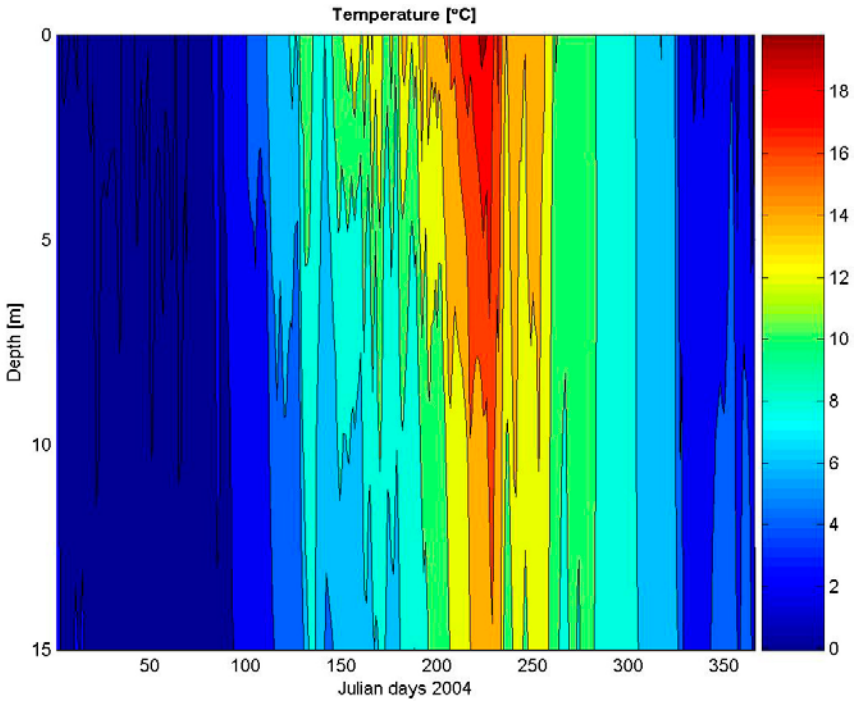

Figure 4-4. *Contours of temperature variations (°C) at the station R-1(Figure 2-2) as computed by the AS3D model /Engqvist and Andrejev 2008/ for 2004.*

4.3 Freshwater discharge

The catchment areas (Table 4-1) of the 13 analyzed time periods have been calculated by Umeå University /SKB 2010a/. Assuming that the specific run-off per unit area is maintained during this entire time period as it took place during 2004 for Laxemarån (Figure 4-5), the discharge to the different SBs can be calculated. This also presupposes that the seasonal variation of the specific run-off of Laxemarån can be inferred from using the 2004 run-off data /Engqvist and Andrejev 2008/ and the corresponding catchment area of the same year.

Table 4-1. Catchment areas (in km²) of the different SBs for the 13 analyzed time periods.

	Catchment areas (km²) of partitioned SBs according to Appendix A														
Time period	B1	B2	B3	B4	B5	B6	B7	B8	B9	B10	B11	B12	B13	B14	B15
3000BC	1.03	19.4	5.23	1.31	24.89	5.30	1.66	3.24	2.82						
2000BC	1.03	19.43	3.06	2.17	0.95	1.83	1.71	36.3	1.60	1.70	0.06				
1000BC	27.0	1.71	0.27	39.6	0.74										
0BC/AD	1.57	3.53	27.3	1.71	2.01	2.83	39.6	1.37	1.86	0.97					
1000AD	35.4	4.34	6.8	41.0	0.35	1.15	1.86	0.97							
2000AD	35.7	35.7	2.3	0.96	0.48	2.83	3.96	0.25	41.0	1.3	0.91	0.63	0.16	2.00	1.26
3000AD	29.2	1.31	2.34	0.33	1.30	43.8	1.66	0.23	0.66	0.92	0.16	3.29			
4000AD	4.94	12.8	1.47	35.7	1.33	0.87	1.28	3.27							
5000AD	35.7	2.61	0.83	1.30	0.17	0.96	0.78	5.77							
6000AD	5.39	0.74	0.42	2.18											
7000AD	6.73														
8000AD	4.76	1.97	0.32	0.91	4.05										
9000AD	4.78	1.95	0.32	0.91	4.05										

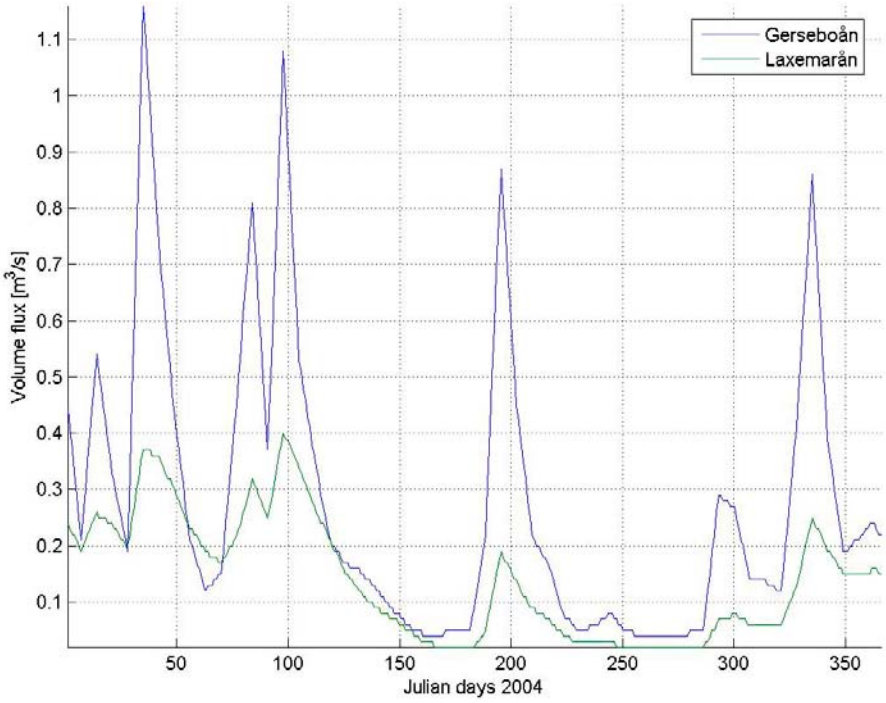

Figure 4-5. *Discharge of the two rivers Gerseboån and Laxemarån during 2004 from /Engqvist and Andrejev 2008/.*

5 Results

First is presented the outcome of the model computation for the various time periods. The 13 analyzed time periods will result in as many *AvA* diagrams. They are all deferred to Figures B-1 through B-13 in Appendix B,

The ambition to treat all potentially involved and contributing basins as objectively as possible meant that a few straits were found to possess a sill height that is close to or even exceeds the culmination (+ 68 cm) of the sea level forcing during the year 2004. Such straits are indicated with an arrow in Figure A-1b through A-13b complementing the standard straight line. The arrow indicates the supposed direction of the water flux. Basins located upstream of an entire set of such straits will not attain a quasi-stationary state regarding its *AvA*-levels within the time span of one year, e.g. BO 205 (or SB B4) for 3000 BC. For iterative one-year runs, the resulting *AvA* will eventually attain a stationary value that, however, will be an order of magnitude longer than one year. It has in such cases been a policy decision to consider such SBs and associated BOs as lakes. This has been indicated in Appendix A with SB boxes filled with a pink color.

5.1 Coastal SB *AvA*

The computation results, comprising mean and standard deviation of the *AvA*-values, are summarized in Table 5-1, where also the respective volumes of the SBs are listed. From these data the associated volume-averaged *AvA*-values of the BO can be calculated for the ones that are subdivided into two or more SBs. The additional SBs (labeled 'New') can now be dismissed since their *AvA*-values have served as contributing to the BOs *AvA*-values that are of interest. For the part of the split BOs that belong to the coastal zone, the *AvA*-value has been temporarily assumed to be zero. This can be adjusted later by merely adding the *AvA*-value of the CZ to be determined, since the volume fraction coefficients when calculating the volume averages remain the same.

If the allotted time frame of the present project had permitted, the sill levels could have been inspected beforehand and then some of the basins could have been omitted from participation in the model computations. This is evident from the SBs that do not reach a quasi-stationary *AvA*-level and applies to BO 205 for 300BC and BOs 201, 203, and 213 for 1000 BC. For 5000 AD, BO 201 is hydraulically disconnected, while for this year and 6000 AD one or two of the SBs into which BO 215 is subdivided has only insignificant water exchange with the CZ.

In Table 5-2 the estimated *AvA*-values with regard to BOs and the 13 different time periods are presented.

Table 5-1. Overview of the resulting *AvA*-data (yearly mean and S.D.) from the model computation of the different SBs, together with their mean volumes. From these data volume averages can be calculated for BOs that are partitioned into two or more SBs shown highlighted in gray. For the part of such BOs that belong to the coastal zone, the *AvA*-value has been temporarily assumed to be zero. The additional SBs (labeled 'New') are left out since their *AvA*-values are of no further consequence. For 2000 BC it may be remarked that the BOs 202 and 203 attain almost identical level of *AvA*, which makes it probable that for 3000 BC they also shared the approximately same *AvA*-levels.

Time period	Sub-Basin (SB)	Biosphere Object (BO)	Volume (1.e6 m^3)	*AvA* mean (days)	*AvA* S.D. (days)
3000 BC	3	202 and 203	9.9	91.3	43.7
3000 BC	6	214	1.0	23.0	3.6
3000 BC		213	2.6	11.4	2.4
3000 BC	7	213_2	0.5	19.7	3.1
3000 BC	8	213_1	2.0	6.5	1.6
3000 BC	9	213_3	0.2	39.1	5.5
2000 BC	3	203	3.2	35.7	13.9
2000 BC	4	202	1.6	35.1	14.8
2000 BC		201	32.5	0.1	1.1
2000 BC	5	201_1	0.1	29.4	17.3
2000 BC	6	205	0.4	11.7	4.3
2000 BC	7	207	1.7	2.0	0.7
2000 BC		213	0.7	39.9	16.4
2000 BC	8	213_2	0.2	39.1	16.4
2000 BC	9	213_1	0.5	40.3	16.5
2000 BC	10	212	0.8	4.4	1.2
2000 BC	11	217	0.0	10.2	2.7
1000 BC		201	16.1	0.2	0.3
1000 BC	1	201_2	0.3	5.3	2.3
1000 BC	3	201_1	0.2	4.8	1.5
1000 BC	2	207	1.0	7.3	2.5
1000 BC	4	212	0.4	3.1	0.7
1000 BC		211	1.0	0.3	0.2
1000 BC	5	211_1	0.2	1.9	0.4
0 BC/AD		201	12.5	2.6	1.3
0 BC/AD	1	201_4	0.1	18.6	6.1
0 BC/AD	2	201_3	2.4	4.3	0.9
0 BC/AD	3	201_1	5.8	3.5	1.0
0 BC/AD	5	201_2	0.1	17.9	9.1
0 BC/AD	4	207	0.7	114.7	26.5
0 BC/AD	6	209	0.3	1.8	0.5
0 BC/AD	7	212	0.1	2.5	0.7
0 BC/AD	8	211	0.5	1.5	0.4
0 BC/AD		216	0.7	4.0	2.0
0 BC/AD	9	216_1	0.5	6.0	2.4
0 BC/AD		215	13.3	0.1	0.2
0 BC/AD	10	215_1	0.1	7.3	1.8
1000 AD		201	9.7	35.2	22.0
1000 AD	1	201_1	9.1	37.5	22.7
1000 AD	3	208	7.0	26.0	9.0
1000 AD	4	211	0.1	14.7	5.4
1000 AD		216	0.3	59.9	33.4
1000 AD	7	216_1	0.2	103.3	43.9
1000 AD		215	9.0	0.003	0.024
1000 AD	8	215_1	0.0	0.6	0.4
2000 AD	1	201	7.7	24.6	13.7
2000 AD	6	209	0.004	19.9	5.6
2000 AD	7	208	4.4	16.2	4.0
2000 AD	9	211	0.1	14.9	4.8
2000 AD	14	216	0.0	40.2	18.4
2000 AD		215	6.1	0.4	0.5
2000 AD	15	215_1	0.7	3.7	1.3

Time period	Sub-Basin (SB)	Biosphere Object (BO)	Volume (1.e6 m³)	*AvA* mean (days)	*AvA* S.D. (days)
3000 AD		201	6.0	63.3	13.1
3000 AD	1	201_1	5.9	61.6	12.9
3000 AD	4	201_2	0.2	78.8	14.8
3000 AD		208	2.9	34.6	6.6
3000 AD	6	208_1	2.9	34.9	6.6
3000 AD	8	208_2	0.04	13.9	4.4
3000 AD		215	4.1	0.2	0.2
3000 AD	12	215_1	0.5	1.5	0.5
4000 AD	4	201	4.6	106	12.9
4000 AD		215	2.6	0.1	0.1
4000 AD	8	215_1	0.2	1.0	0.3
5000 AD		215	1.6	3.5	2.0
5000 AD	8	215_2	1.6	3.5	1.4
6000 AD		215	0.9	8.1	4.1
6000 AD	1	215_2	0.0	21.6	14.8
6000 AD	2	215_1	0.9	7.3	2.2
6000 AD	4	215_4	0.0	26.5	20.1
7000 AD	1	215	0.6	5.8	1.7
8000 AD		215	0.4	23.4	6.0
8000 AD	1	215_2	0.2	24.2	6.3
8000 AD	2	215_1	0.2	22.4	5.7
9000 AD		215	0.2	47.3	11.8
9000 AD	1	215_2	0.1	48.6	13.3
9000 AD	2	215_1	0.1	46.1	10.1

Table 5-2. *AvA* expressed in days for the 16 BOs calculated from *AvA*-values computed from the maximally 15 SBs in Table 3-1. Numbers in red figures denote *AvA* (days) directly computed results by the *CouBa* model. Numbers in blue figures denote *AvA* (days) as inferred volume averages of partitioned coastal basins computed by model.

Biospere object (BO)	3000 BC	2000BC	1000 BC	0 BC/AD	1000 AD	2000 AD	3000 AD	4000 AD	5000 AD	6000 AD	7000 AD	8000 AD	9000 AD
CZ													
201		0.1	0.2	2.6	35.2	24.6	63.3	106.1					
202	91.3	35.1											
203	91.3	35.7											
204													
205		11.7											
206													
207		2.0	7.3	114.7									
208					26	16.2	34.6						
209				1.8		19.9							
210													
211			0.3	1.5	14.7	14.9							
212		4.4	3.1	2.5									
213	11.4	39.9											
214	23.0												
215				0.1	0.003	0.4	0.2	0.1	3.5	8.1	5.8	23.4	47.3
216		10.2		4.0	59.9	40.2							

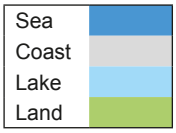

5.2 Coastal Zone *AvA*

The *AvA* of the coastal zone must also to be estimated. Since this *AvA*-value has hitherto tacitly been assumed to be zero, a higher assumed value would additively increase the total *AvA*-values of the connected coastal basins. The method to arrive at one such appreciation is to apply four different methods and choose the least favorable one, i.e. the one with greatest *AvA*-value of these.

The average velocity for the years 3000 BC and 1000 BC of the Forsmark open coastal water (length-scale about 5.5 km) is 2.9 and 3.9 cm/s respectively /Karlsson et al. 2010/ which gives a mean *AvA* of 2.2 days. Assuming the same average current in the Laxemar-Simpevarp region, the off-shore coastal basin of Laxemar (i.e. BO 20) is approx. 10 km which results in the highest *AvA* of about 3.8 days for 3000 BC.

Measurement of the N/S-current component /Engqvist and Andrejev 2008/ at a coastal station (Si21) in the vicinity of station R-1 (see Figure 2-2) during 2004 gives –2 cm/s (average with regard to sign) and 6 cm/s (absolute average with no regard to sign), Figure 5-1. An *AvA* estimate based on a time-constant large-scale through-flow in the N/S-direction would then amount to 5.8 days. The concomitant spectrum variance is, however, less than 3 days for surface currents, which means that the time-varying components of the flow field also should contribute. The corresponding flow components in the E/W-direction are also small (meaning slow through-flow in this direction) but nevertheless amount to more than half of the N/S-component. Since the length-scale in the E/W direction is about one quarter than that of the N/S-direction, this component of water exchange certainly contributes to lowering the *AvA*-measure. Considering both these additional factors, a conservative *AvA*-value of 4 days would be a safe conservatively estimated yearly average.

The *AvA* of the CZ was computed with forcing pertaining to 1981 to be 1.85 ± 0.8 days using the AS3D-model /Engqvist 2006/. Basin 15 in the same study bears a strong similarity to the CZ for 2000 AD of the present study. By using the same 3D model approach, the *AvA* for this basin was calculated to be a mere 0.58 ± 0.2 days.

The surface-most current in Figure 5-1 is consistently stronger and in combination with a generally sloping bottom profile in the off-shore direction, and it seems safe to assume that as the land rise progresses, the ventilation of the coastal zone would remain mainly the same. This certainly presupposes that the weather forcing is mainly invariant during the studied period 3000 BC through 9000 AD.

These four different estimates are summarized in Table 5-3. Giving measurement-based data the most weight when determining an *AvA*-value for the CZ, a value that should not be expected to be exceeded during the time period 3000 BC to 9000 AD would then be 4 days.

Adding the mean and S.D. of the CZ to the estimated *AvA*-values in Table 5-3, the final results are presented in Table 5-4, in which the last two columns with the combined *AvA*-estimates expressed as fraction of one year, represent the data that have been passed on to the ensuing Pandora model computations (the Radionuclide model, see chapter 10 in /Andersson 2010/).

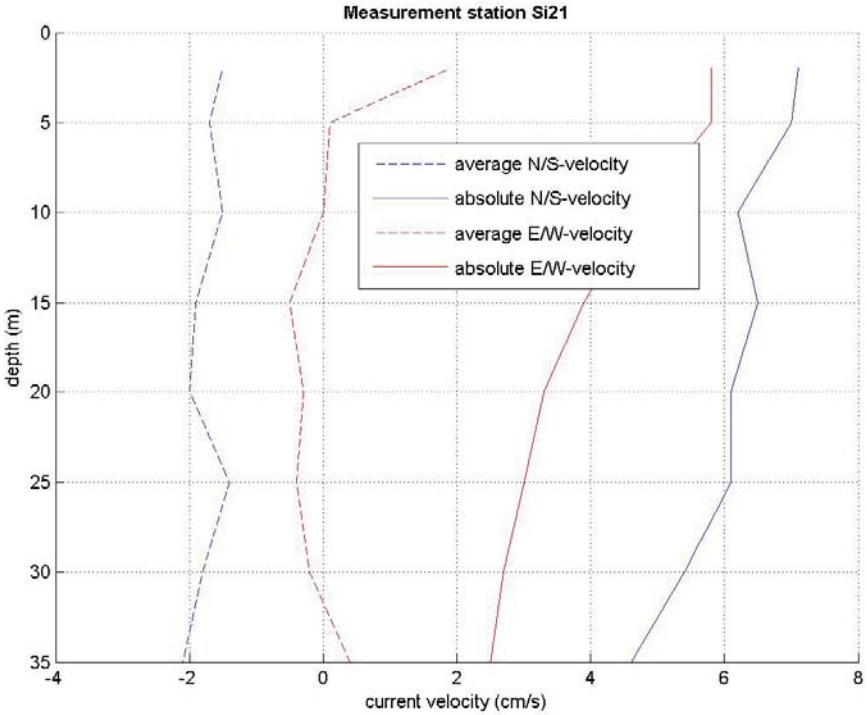

Figure 5-1. *Statistical properties of measured current components at the offshore coastal station Si21 in the vicinity of station R-1 in Figure 2-2.*

Table 5-3. Presentation of four different estimates of AvA-times concerning the coastal zone. The highest of these estimates has been chosen.

Area	Area type	Period	Basis of estimate	*AvA* (days)	S.D. (days)
Forsmark	Open coast	3000 BC	Average computed velocity	3,8	–
Laxemar	Station Si21	2004	Average measured velocity	4,0	2,0
Laxemar	CZ	1981	Average computed velocity	1,8	0,8
Laxemar	Basin 15	1981	Average computed velocity	0,6	0,2

Table 5-4. Overview of residence times expressed as AvA-estimates. The values in the two last columns are converted to fractions of year and have been passed on to the Pandora dose computations.

		Land-locked basins		Coastal zone		Combined	
Period	Basin object (BO)	AvA mean (days)	AvA S.D. (days)	AvA mean (days)	AvA S.D. (days)	AvA mean (years)	AvA S.D. (years)
3000 BC	202 and 203	91.3	43.7	4.0	2.0	0.261	0.120
3000 BC	214	23.0	3.6	4.0	2.0	0.074	0.011
3001 BC	213	11.4	2.4	4.0	2.0	0.042	0.009
2000 BC	203	35.7	13.9	4.0	2.0	0.109	0.038
2000 BC	202	35.1	14.8	4.0	2.0	0.107	0.041
2000 BC	201	0.1	1.1	4.0	2.0	0.011	0.006
2000 BC	205	11.7	4.3	4.0	2.0	0.043	0.013
2000 BC	207	2.0	0.7	4.0	2.0	0.016	0.006
2000 BC	213	39.9	16.4	4.0	2.0	0.120	0.045
2000 BC	212	4.4	1.2	4.0	2.0	0.023	0.006
2000 BC	217	10.2	2.7	4.0	2.0	0.039	0.009
1000 BC	201	0.2	0.3	4.0	2.0	0.011	0.006
1000 BC	207	7.3	2.5	4.0	2.0	0.031	0.009
1000 BC	212	3.1	0.7	4.0	2.0	0.019	0.006
1000 BC	211	0.3	0.2	4.0	2.0	0.012	0.005
0 BC/AD	201	2.6	1.3	4.0	2.0	0.018	0.006
0 BC/AD	207	114.7	26.5	4.0	2.0	0.325	0.073
0 BC/AD	209	1.8	0.5	4.0	2.0	0.016	0.006
0 BC/AD	212	2.5	0.7	4.0	2.0	0.018	0.006
0 BC/AD	211	1.5	0.4	4.0	2.0	0.015	0.006
0 BC/AD	216	4.0	2.0	4.0	2.0	0.022	0.008
0 BC/AD	215	0.1	0.2	4.0	2.0	0.011	0.006
1000 AD	201	35.2	22.0	4.0	2.0	0.107	0.060
1000 AD	208	26.0	9.0	4.0	2.0	0.082	0.025
1000 AD	211	14.7	5.4	4.0	2.0	0.051	0.016
1000 AD	216	59.9	33.4	4.0	2.0	0.175	0.092
1000 AD	215	0.003	0.024	4.0	2.0	0.011	0.005
2000 AD	201	24.6	13.7	4.0	2.0	0.078	0.038
2000 AD	209	19.9	5.6	4.0	2.0	0.066	0.016
2000 AD	208	16.2	4.0	4.0	2.0	0.055	0.012
2000 AD	211	14.9	4.8	4.0	2.0	0.052	0.014
2000 AD	216	40.2	18.4	4.0	2.0	0.121	0.051
2000 AD	215	0.4	0.5	4.0	2.0	0.012	0.006
3000 AD	201	63.3	13.1	4.0	2.0	0.184	0.036
3000 AD	208	34.6	6.6	4.0	2.0	0.106	0.019
3000 AD	215	0.2	0.2	4.0	2.0	0.011	0.005
4000 AD	201	106.1	12.9	4.0	2.0	0.301	0.036
4000 AD	215	0.1	0.1	4.0	2.0	0.011	0.005
5000 AD	215	3.5	2.0	4.0	2.0	0.021	0.008
6000 AD	215	8.1	4.1	4.0	2.0	0.033	0.013
7000 AD	215	5.8	1.7	4.0	2.0	0.027	0.007
8000 AD	215	23.4	6.0	4.0	2.0	0.075	0.017
9000 AD	215	47.3	11.8	4.0	2.0	0.140	0.033

6 Discussion

It may seem somewhat disturbing from Table 3-1 that the most complex basin and strait configuration occurs for contemporary times. A possible and plausible explanation would be that the nuclear reactors must be located near the present time shoreline to arrange for the cooling. This in turn has decided the location of the repository and the estimated exit holes occurring in the vicinity of this site and from their location the actual BOs are defined. This expression of a seeming bias for contemporary times also applies to the analogous investigation the Forsmark area /SKB 2010b/.

The inclusion of SBs that are connected to straits whose sill height exceed the peak of sea-level forcing is less problematic. Normally the run-off water is considered exogenous with *AvA*-value zero. The downstream basins will – as a consequence of the inclusion – receive more aged water, thus increasing their own *AvA*-value, which is consistent with the general policy of avoiding underestimations.

6.1 Morphometrical succession

The succession from open sea, coastal SB, lake and finally land can be clearly seen in Table 5-2. For two BOs (209 and 216) this order is broken by an ensuing lake between two coastal SBs in time succession. This is because different parts of the respective BO become connected to the coastal zone as the land rises. One would *a priori* expect a progression with steadily increasing *AvA*-values as for BO 207, but the evolution of SB volumes and the corresponding strait cross-sections together with altered run-off pathways is sufficiently complicated to also comprise retrograde development, e.g. for BO 201 displaying a local minimum *AvA*-value for 4000 AD.

6.2 Uncertainty due to hypsography

In spite of the pronounced ambition to treat all derivations of the hypsographic data as similarly and objectively as possible, there are many possible sources of errors in addition to the finite resolution of the DEM which only for 2000 AD is possible to compare with an almost independent data set. The configuration shown in Figure 3-49 in /Engqvist 2006/, reveals both similarities and differences compared to the corresponding one in Figure A-6b. Some of the SBs in the former study were in addition to being derived from a DEM also based on *in situ* soundings. In particular this applies to the narrow straits that both the present and the former DEMs resolve poorly. Some of the basins of these two studies are sufficiently close counterparts, so a direct comparison of their *AvA*-values offers a way to assess the overall inaccuracy with regard to the hypsographic aspect. This is achieved by running the present version of the **CouBa**-model with the configuration and hypsographical features of the former study /Engqvist 2006/[1] and after adjusting the *AvA* volume averages of the former SBs so that they correspond to as a close match as possible to the present ones. The result is presented in Table 6-1. A corresponding scatter plot of the same *AvA*-values of the six compared SBs is depicted in Figure 6-1. The correlation coefficient is 0.95. The slope of the regression line for the average values is about 40% less than unity, meaning that in the present study the mean *AvA*-values are comparatively underestimated relative to what was found in the former study. This is unfortunately not consistent with the given guidelines to avoid overestimations of the rate of water exchange since this translates into possible underestimations of the ensuing dose computations. Since it cannot be determined which of these two studies is the more realistic one, it must be concluded that there is an uncertainty of the same degree concerning the overall methodology in deriving the bathymetric data.

6.3 Uncertainty due to climatology

Even though it could be argued that the aberration due to hypsography is mitigated by the inadvertent inclusion of hydraulically disconnected basins, there are other sources of uncertainty. /Engqvist 2006/ performed a sensitivity analysis in which not only the hypsographic data (varying basin areas and

[1] This study was run with forcing pertaining to 1981 and thus cannot be used for a fair comparison.

strait cross-section areas) but also ± 10% perturbations of the forcing factors (run-off, wind speed, boundary and sea level fluctuations) were studied, all together eight different factors. It was found that reducing basin areas and the run-off intensity meant a reduced *AvA* of almost the same magnitude, averaged over the total water volume of all twelve comprised SBs. Likewise it was shown that adding a high-frequency component to the sea level forcing also lowered the mean *AvA*-level twice this amount. Notwithstanding this analysis, there is reason to believe that the climatologically induced variations during the 12 thousand years that the present study spans are less than the seasonal variations during 2000 AD, which standard deviations are listed in Table 5-4. A first but conservative worst case appreciation of the uncertainty due to climate variations would then be to subtract 1 S.D. from the mean *AvA*-values and assess the corresponding slope, which is done in Figure 6-1. This slope is close to 1/3, making a conservative estimate of the overall uncertainty a factor 3.

Table 6-1. Comparison of the actual configuration layout (Figure A-6b) vs. the configuration deduced in an earlier study (Figure 3-49, p.121 in /Engqvist 2006/) and their consequences for the *AvA*-estimates. Only the presented pairs of basins that correspond to a sufficiently close area-wise match have been included in this table. The mean *AvA*-estimates in red bold numbers serve as a reasonable basis for a valid comparison.

Present SB number	Biospere object (BO)	Mean *AvA* (days)	S.D. *AvA* (days)	Former SB number	Mean *AvA* (days)
B1	201	24.6	13.7	b2	37.0
B2	Ny_2	11.2	4.7	b12	15.0
B3	Ny_1	6.6	2.9	b6	10.7
B4	Ny_3	16.8	7.8	b5	32.8
B7	208	16.2	4.0	b1	32.2
B15	215_1	3.7	1.3	b14	2.0

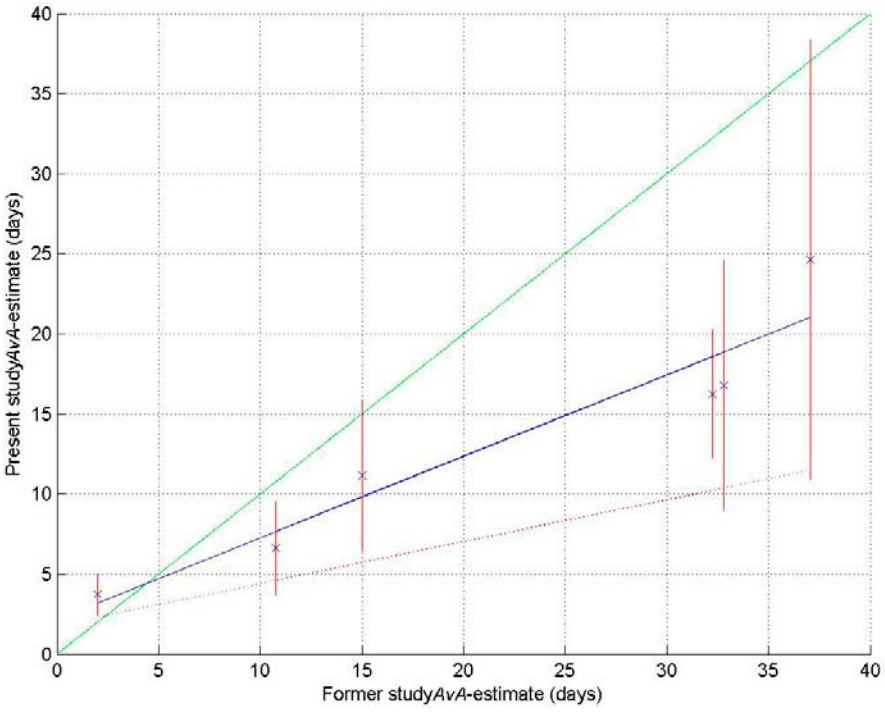

Figure 6-1. *Scatter diagram showing the AvA-values of the present and former configuration SBs. The present study's strait hypsographic data are entirely based on DEM in combination with computed sedimentation processes, the former data are to a certain extent also based on soundings. The blue solid regression line involves all SBs that are deemed as sufficiently similar with regard to their horizontal delimitation to be pairs of a valid comparison. The red bars denote the S.D. of the present data and the red dotted line the same data set minus 1 S.D. The slope of both regression lines is smaller than the diagonal equivalence line in green and amounts to approximately 1/3 for the latter line.*

7 Summary and conclusions

The retention time expressed as *AvA* for the 16 analyzed sequentially occurring water bodies of the BOs have been estimated for the 13 time periods from 3000 BC to 9000 AD equally interspersed 1,000 years apart in time. The hypsographic data and catchment areas estimates have been extracted from an enhanced DEM subjected to a sedimentation model /SKB 2010a/. Great care has been taken to make the inferred subdivision and the derivation of the basin and strait hypsographic curves as objective as possible. In choice situations the one that is deemed to lead to an overestimation of the *AvA*-values has been generally chosen.

The unique possibility to check the present results with the *AvA*-estimates of another study occurs for contemporary times, i.e. 2000 AD, and indicates that an undesired underestimation bias may have been achieved amounting to 40% relative to a former study. On top of this level of uncertainty must be added also the contribution of the uncertain climate variations. A first but safely conservative appreciation of the overall uncertainty would depart from a worst-case scenario, namely that the climate variations are in parity with the seasonal variations during 2000 AD. This yields an uncertainty factor 3 for a possible 1 S.D. overestimation of the water exchange.

8 Acknowledgements

Without the kind and dedicated assistance of Lars Brydsten and Mårten Strömgren, both affiliated to Umeå University, with extraction of specified GIS-data, this project could not have been completed within the short time-frame allotted. Also a nonymous internal reviewer, Karin Aquilonius, has improved the readability of the manuscript considerably. I thus extend my sincere gratitude to all three of these contributors for their forthcoming and excellent cooperation.

9 References

SKB's (Svensk Kärnbränslehantering AB) publications can be found at www.skb.se/publications.

Andersson E (ed), 2010. The limnic ecosystems at Forsmark and Laxemar-Simpevarp. SR-Site Biosphere. SKB TR-10-02, Svensk Kärnbränslehantering AB.

Brydsten L, Strömgren M, 2005. Digital elevation models for site investigation programme in Oskarshamn. Site description version 1.2. SKB R-05-38, Svensk Kärnbränslehantering AB.

Dalziel S B, 1992. Maximal exchange in channels with nonrectangular cross sections. Journal of Physical Oceanography, 22, pp 1188–1206.

Deleersnijder E, Campin J-M, Delhez E, 2001. The concept of age in marine modelling I. Theory and preliminary model results. Journal of Marine Systems, 28, pp 229–267.

England M H, 1995. The age of water and ventilation timescales in a global ocean model. Journal of Physical Oceanography, 25, pp 2756–2777.

Engqvist A, 1996. Self-similar multi-layer exchange flow through a contraction. Journal of Fluid Mechanics, 328, pp 49–66.

Engqvist A, 1997. Water exchange estimates derived from forcing for the hydraulically coupled basins surrounding Äspö island and adjacent coastal water. SKB TR 97-14, Svensk Kärnbränslehantering AB.

Engqvist A, 2006. Coastal oceanography of the Laxemar area. Chapter 3.5. In: Lindborg T (ed). Description of surface systems. Preliminary site description Laxemar subarea – version 1.2. SKB R-06-11, Svensk Kärnbränslehantering AB, pp 113–139.

Engqvist A, Andrejev O, 2008. Validation of coastal oceanography at Laxemar-Simpevarp. Site descriptive modeling, SDM-Site Laxemar. SKB TR-08-02, Svensk Kärnbränslehantering AB.

Engqvist A, Stenström P, 2004. Archipelago Strait Exchange Processes – An overview. Deep Sea Research Part II: Topical Studies in Oceanography, 51, pp 371–392.

Engqvist A, Stenström P, 2009. Flow regimes and long-term water exchange of the Himmerfjärden estuary. Estuarine, Coastal and Shelf Science, 83, pp 159–174.

Engqvist A, Döös K, Andrejev O, 2006. Modeling water exchange and contaminant transport through a Baltic coastal region. AMBIO: A Journal of the Human Environment, 35, pp 435–447.

Karlsson A, Eriksson C, Borell Lövstedt C, Liungman O, Engqvist A, 2010. High-resolution hydrodynamic modelling of the marine environment at Forsmark between 6500 BC and 9000 AD. SKB R-10-09, Svensk Kärnbränslehantering AB.

SKB, 2010a. Comparative analysis of safety related site characteristics. SKB TR-10-54, Svensk Kärnbränslehantering AB.

SKB, 2010b. Biosphere analyses for the safety assessment SR-Site – synthesis and summary of results. SKB TR-10-09, Svensk Kärnbränslehantering AB.

Appendix A

Shoreline maps and discrete coupled basin configurations of land-locked basins of the Laxemar-Simpevarp area 3000 BC through 9000 AD

The conventions for specifications of the cartographic information in order to assess the hypsographic features of the basins and straits have been outlined in Chapter 3.3. These data give the area and the width of a strait for every meter of depth from 1 m above the MW-level down to the bottom utilizing the actual DEM /Brydsten and Strömgren 2005/ complemented with computed sediment transport modification of the bathymetry as was performed for the Forsmark area /SKB 2010a/.

The depicted shorelines are for all 13 time periods one meter above the MW, while the peak of sea level of the used 2004 data does not reach higher than 68 cm. This means that for some straits the rendered shoreline somewhat overstates the width. In turn this means that a few straits and adjacent basins could have been dismissed from participating in the model computations since such straits are inherently blocked from taking part in a two-way exchange. The maps and their concomitant subdivision into discrete basin configurations are presented in pairs.

Due to restricted graphical resolution, the (blue broken) delimitation lines shown in the maps cannot in some cases give more than a rough indication of the actually used separation lines, which have been selected using the full resolution of the DEM. For the deduced configuration, the number of straits and basins is presented. According to a topological theorem (going back to Leonhard Euler in the 18th century), their difference gives the number of internal circulation loops. This provides a quick method of checking the consistency. An overview of these configuration features is presented in Table 3-1.

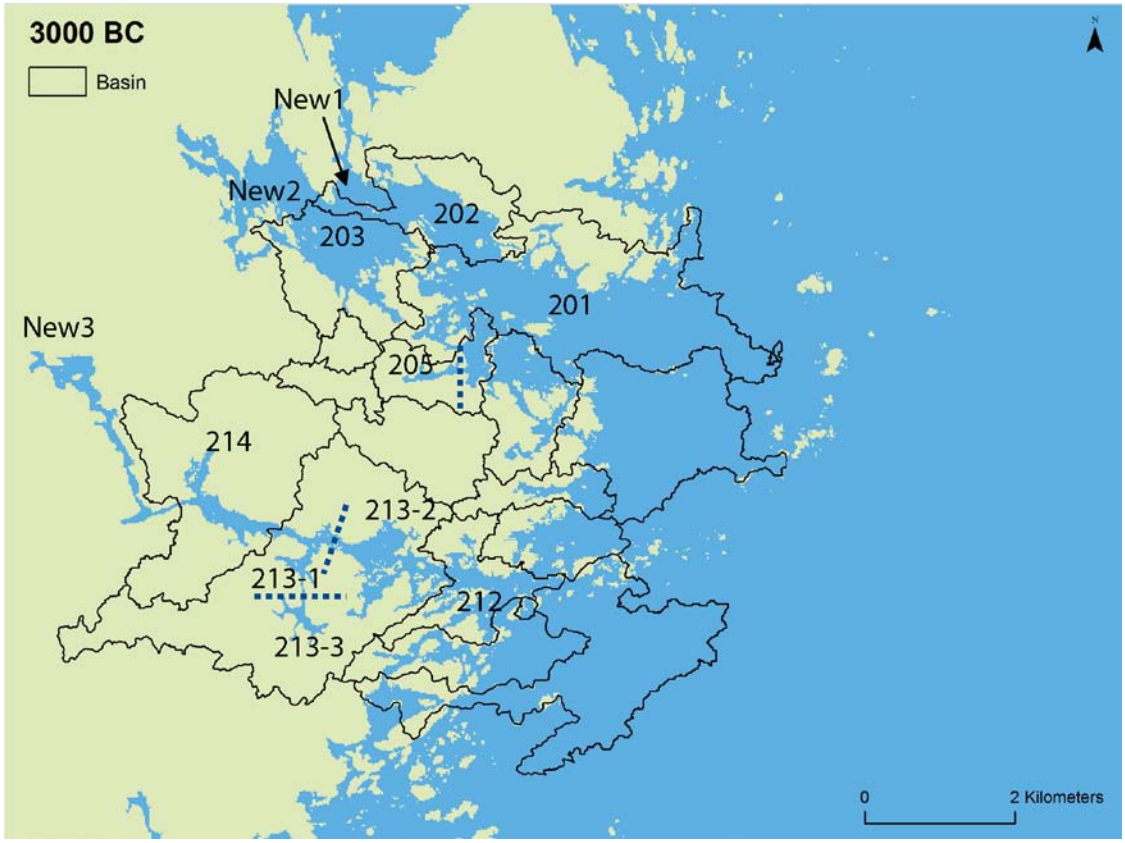

Figure A-1a. *Delimitation of the coastal basins with the shoreline of the year 3000 BC. Three new basins that extend inland are necessary to include. Basins 202 and 203 have been conjoined into one resulting basin named B3 in Figure A-1b. Basin 205 is split along a strait and the outer section (designated 205-0) is considered to belong to the open CZ together with 201 and 212 and the open coastal basins in between. Basin 213 is partitioned into three sections. These latter subdivisions are indicated with broken blue lines.*

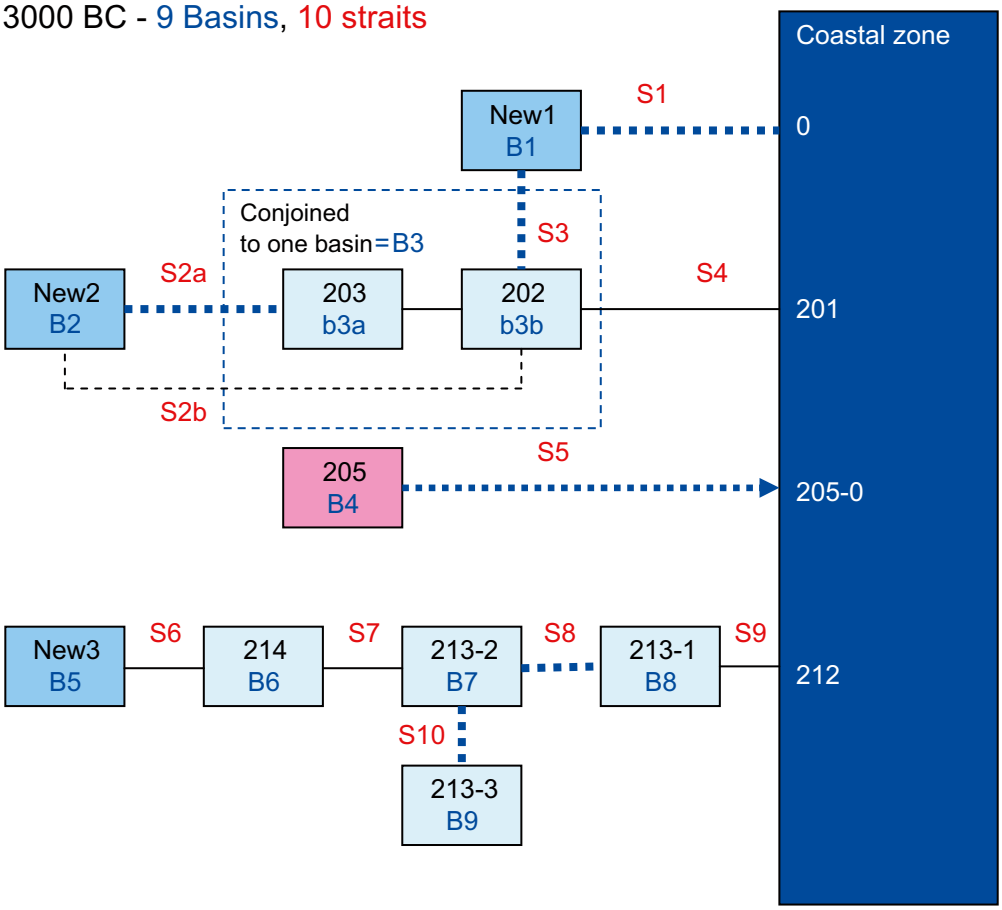

Figure A-1b. *Resulting coupled discrete basin configuration with the interconnecting straits enumerated in systematic order. The straits that do not coincide with BO interfaces are marked with broken blue lines. Also note that the conjunction of BO 202 and 203 – motivated by the wide strait separating them – results in two interfaces (from New2 to 203 and 202 respectively) via straits S2a and S2b, of which the section area of the former strait clearly dominates over the latter. The strait S5 was entered into the modeled configuration but its sill height was subsequently found to exceed the peak of the sea level forcing and is thus hydraulically blocked from participating in the water exchange. The sub-basin B4 (BO 205) could thus have been omitted from the model computation, which in hindsight has been indicated by pink filling color. The '0' in the Coastal Zone represents the open water north of the New1 basin.*

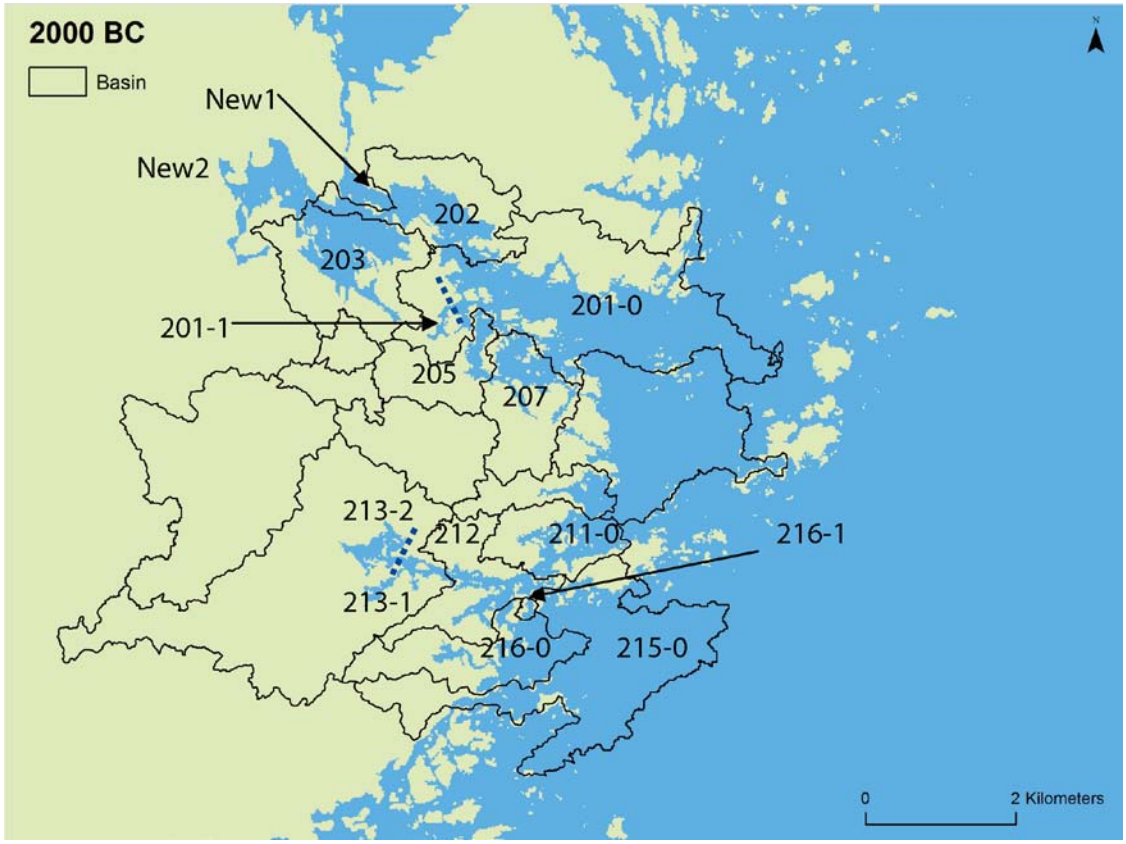

Figure A-2a. *Delimitation of the coastal basins with the shoreline of the year 2000 BC. Two new basins that extend inland need to be included. There is no motivation for the BOs 202 and 203 to be conjoined since the interfacial strait has shrunk with the land rise. Note that between the BO 202 and New2 there is formally a strait but its sill is above the highest peak of the sea level fluctuation for the 2004 forcing. A small branch of BO 201 is deemed sufficiently secluded and land-locked to merit an accounting as a SB. The outer part of this BO (201-0) interfaces with BO 205 and 207 along curved line interspersed with small islands. BO 213 has been split into two SBs and the sea-most exit to the open coast via BO 215 and 216 which are marked with a trailing '0' to indicate that they are considered to belong to the CZ. The meandering embayment near the center of BO 216 is not considered a valid SB since it is not associated with any exit points and connects directly to the CZ.*

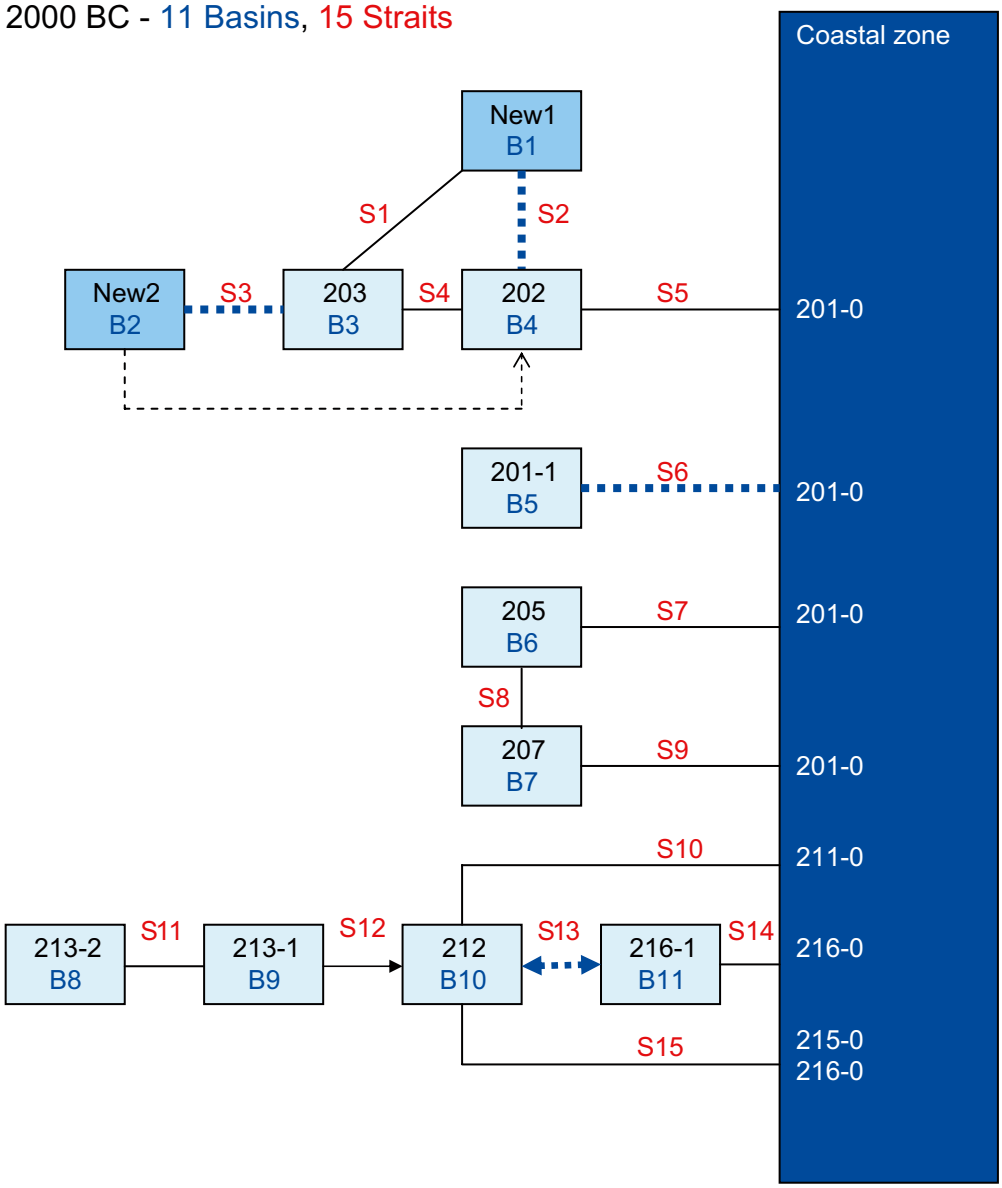

Figure A-2b. *Resulting coupled discrete basin configuration with the interconnecting straits enumerated in systematic order. The straits that do not coincide with BO interfaces are marked with broken blue lines. The strait between New2 and BO 202 has a sill level that exceeds the highest sea level of the forcing and can thus be discarded, which is indicated by the broken black line. BO 212 possesses two strait connections to the open CZ in addition to the strait connecting it to BO 216-1, whose sill level is too elevated to permit simultaneous two-way water exchange. However, run-off water may flow in either direction during different time periods.*

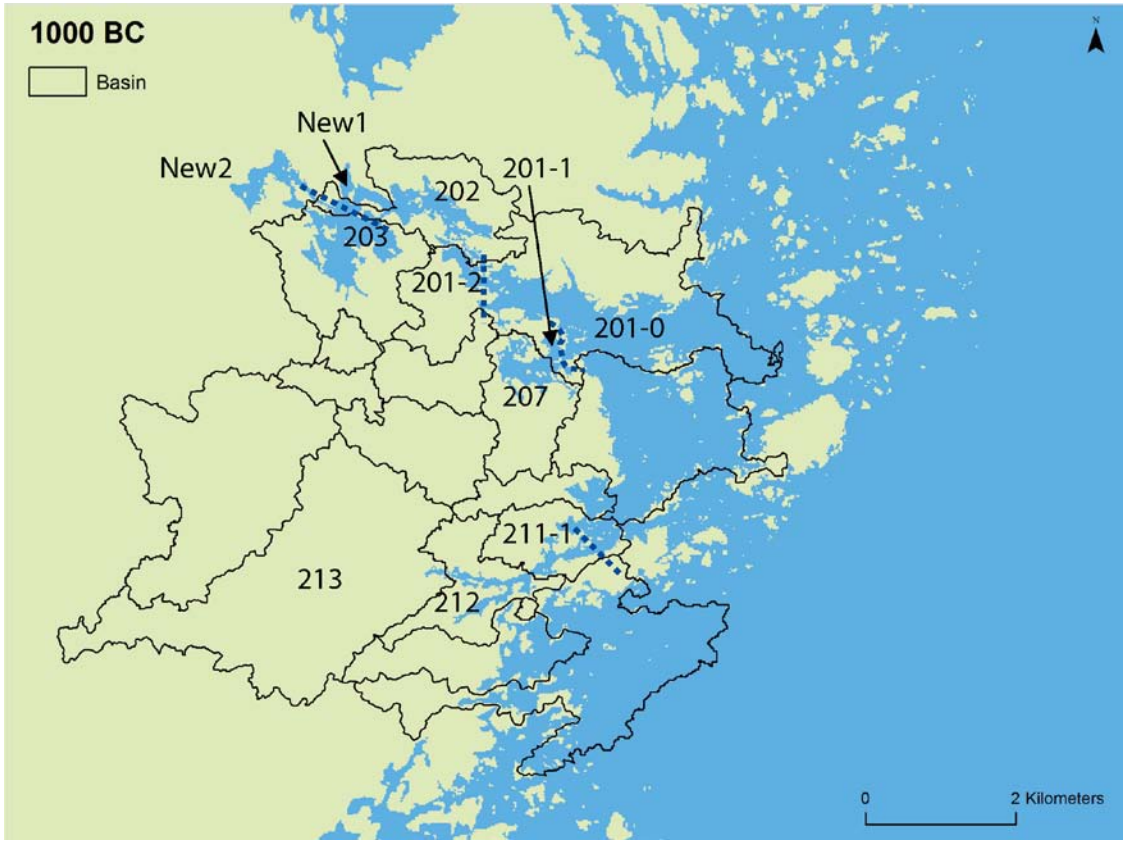

Figure A-3a. *Delimitation of the coastal basins with the shoreline of the year 1000 BC. Two new basins that extend inland seem to still need to be included. It is revealed, however, when inspecting the resulting sill level between the BOs 202 and 201-2 that this is higher than peak of the forced sea level, which means that the inland basins are hydraulically decoupled. This also applies to the minute fjord branch that protrudes into BO 213.*

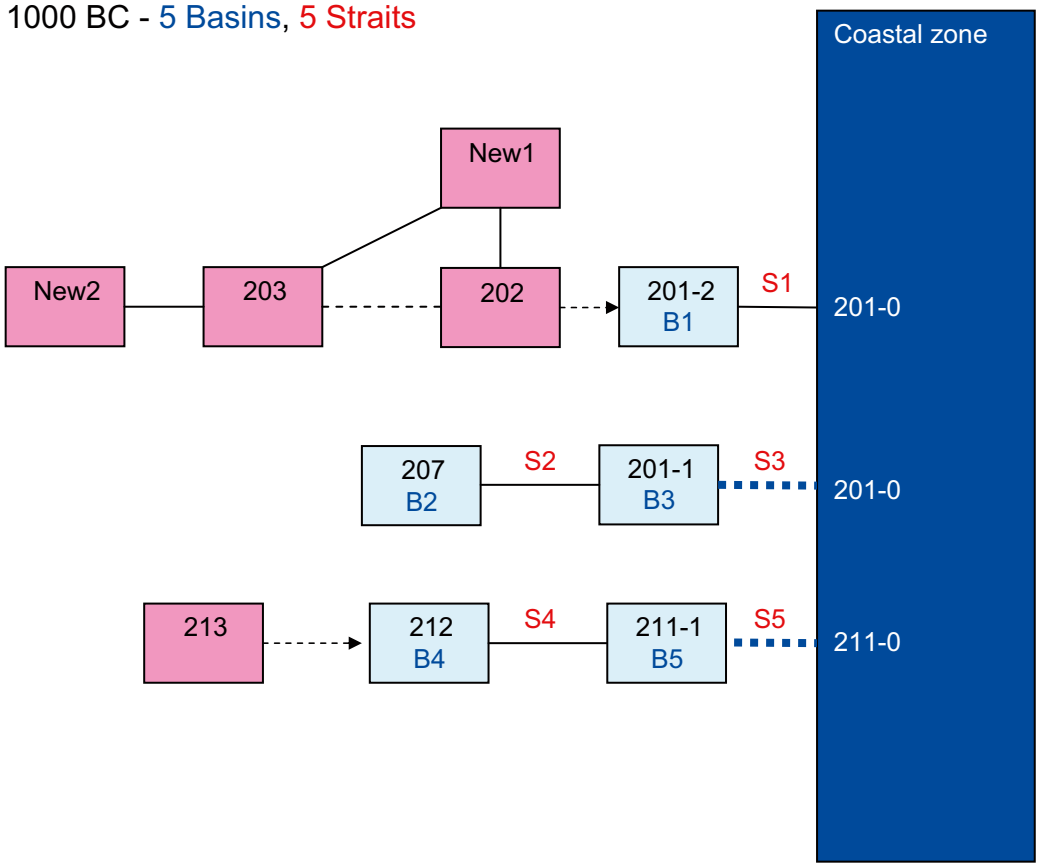

Figure A-3b. *Resulting coupled discrete basin configuration with the interconnecting straits enumerated in systematic order. The straits that do not coincide with biosphere basin interfaces are marked with broken blue lines. The strait between the BOs 202 and 201-2 has a sill level that exceeds the highest sea level of the forcing and can thus be discarded, which is indicated by the broken black line with an arrow connecting them. This thus dismisses all the SBs located upstream, which is indicated by pink filling color. Only run-off water flows in the indicated direction in the straits marked with an arrow.*

Figure A-4a. *Delimitation of the coastal basins with the shoreline of the year 0 BC or AD. No new basins need to be included. BO 201 is subdivided into five sections of which the sea-most is consequentially named 201-0. BO 211 represents a land-locked basin but as it and its fjord arms that extend into BO 212 is not associated with any exit points, these basins have been excluded from being subjected to the model. The strait 201-1/201-0 may seem as an arbitrary designated interface but will be more clearly motivated as the land rises in the following time periods.*

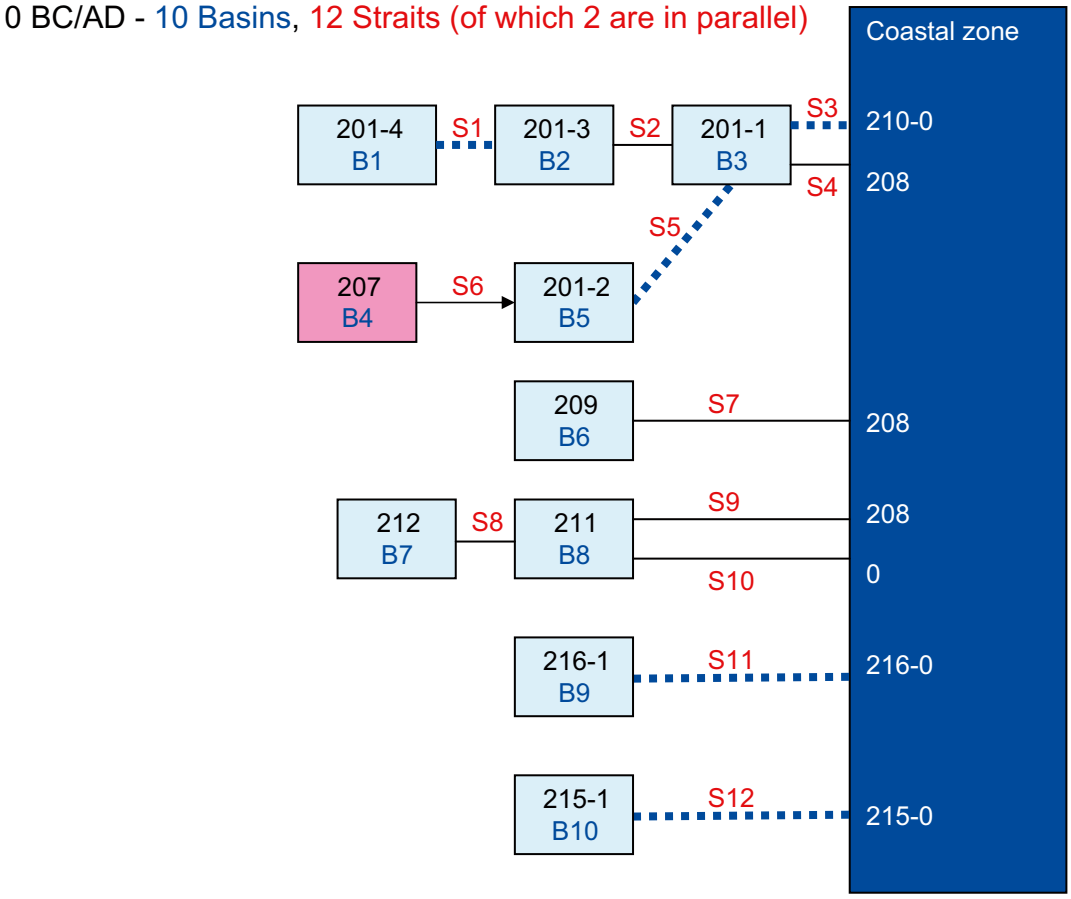

Figure A-4b. *Resulting coupled discrete basin configuration with the interconnecting straits enumerated in systematic order. The straits that do not coincide with biosphere basin interfaces are marked with broken blue lines. Discounting the two occurrences of the two straits in parallel there are no internal circulation loops. Only four straits are not coincidental with the interfaces of the BO basins. Strait S6 turned out to be too shallow for a two-way exchange, which was only noted after it and BO 207 had been subjected to model computation.*

Figure A-5a. *Delimitation of the coastal basins with the shoreline of the year 1000 AD. Three new basins needed to be added. SB New1 has several strait connections to BO 201 and 208 and its elongated character is rendered by presenting (but not computing) it as three SBs. New1a through New1c. For practical computing reasons the SB New1b which consists of the outer part of BO 201 (coincidental with 201-0) has thus been treated as conjoined with the other two fjord branches of SB New1. The arising small embayment indicated by a red circle has been omitted because it is not associated with any exit points.*

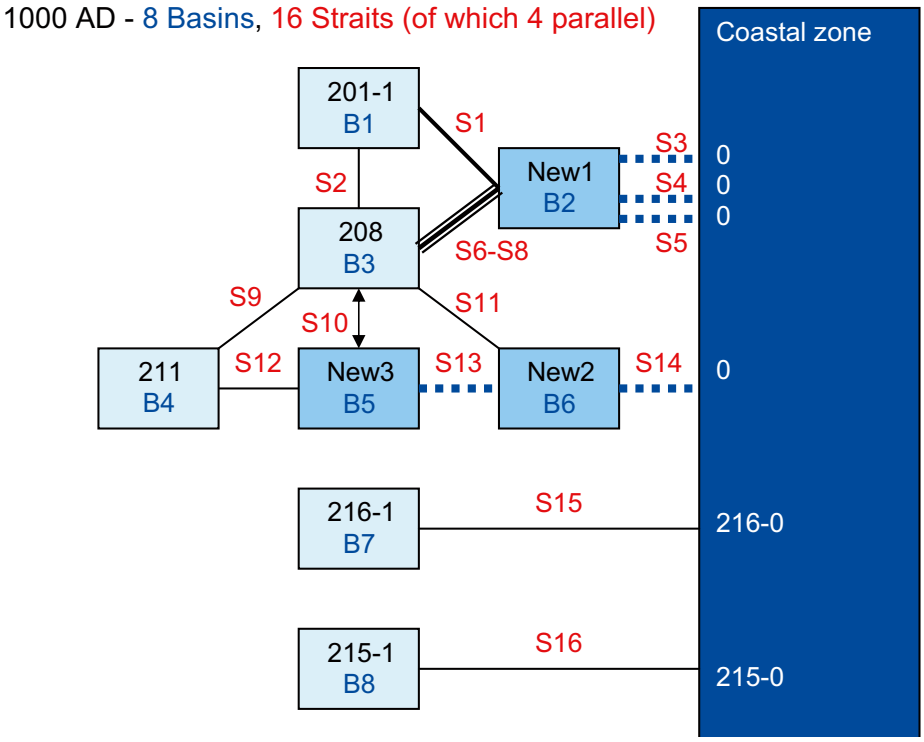

Figure A-5b. *Resulting coupled discrete basin configuration with the interconnecting straits enumerated in systematic order. The straits that do not coincide with biosphere basin interfaces are marked with broken blue lines. Discounting the two occurrences of the two straits in parallel there are no internal circulation loops. Only five straits are not coincidental with the interfaces of the biosphere object basins. The '0' in the Coastal zone box represents the nondescript CZ. The strait S10 was entered into the modeled configuration but its sill height was subsequently found to exceed the peak of the sea level forcing and has thus been hydraulically blocked from participating in simultaneous two-way water exchange. The forced run-off water in the model can, however, flow in both directions depending on which of BO 208 and SB New3 possess the lower sea level at a given time.*

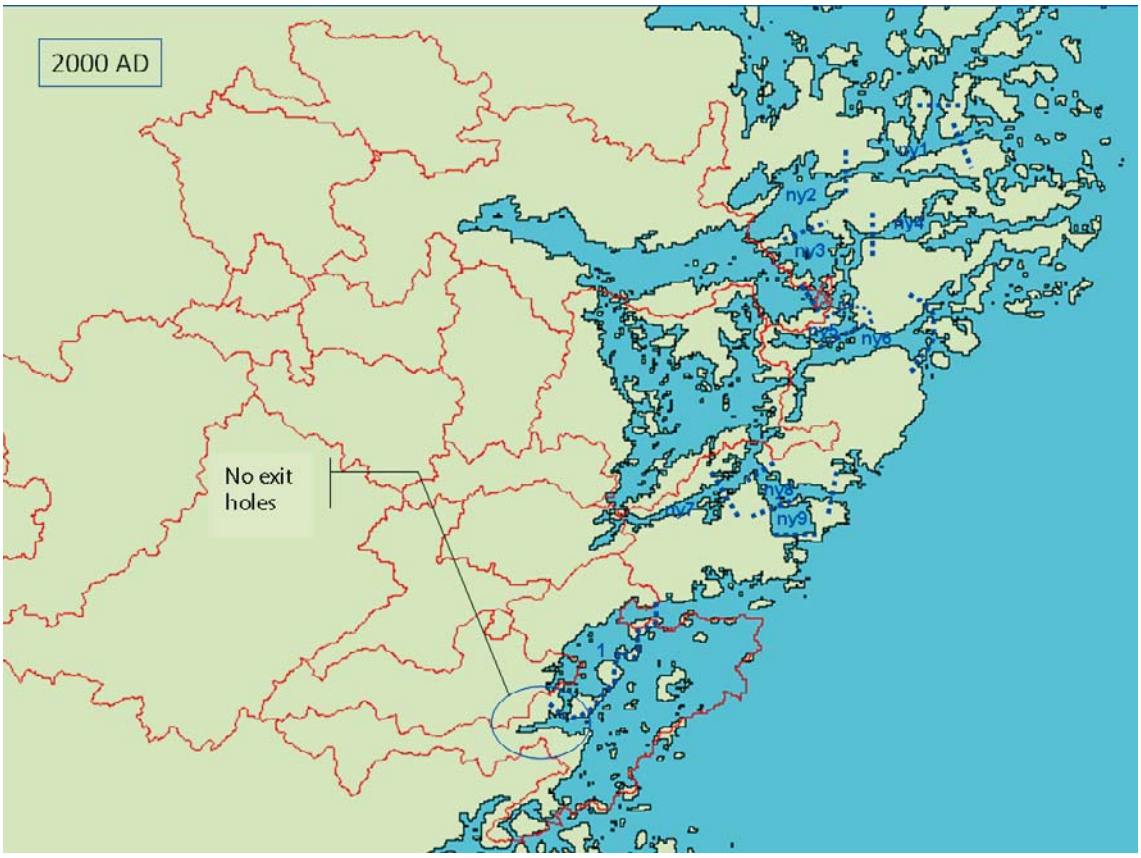

Figure A-6a. *Delimitation of the coastal basins with the shoreline of the year 2000 AD. The straits that do not coincide with BO-interfaces are marked with broken blue lines. As the land rises, nine additional SBs are needed towards the CZ in order to make the water exchange realistic. For graphical space reasons these additional SBs have been indicated with with 'ny' instead of 'new'. The southern occurring embayment of BO 215 (marked with a blue oval) has been omitted from the model computations since it is not associated with any exit points.*

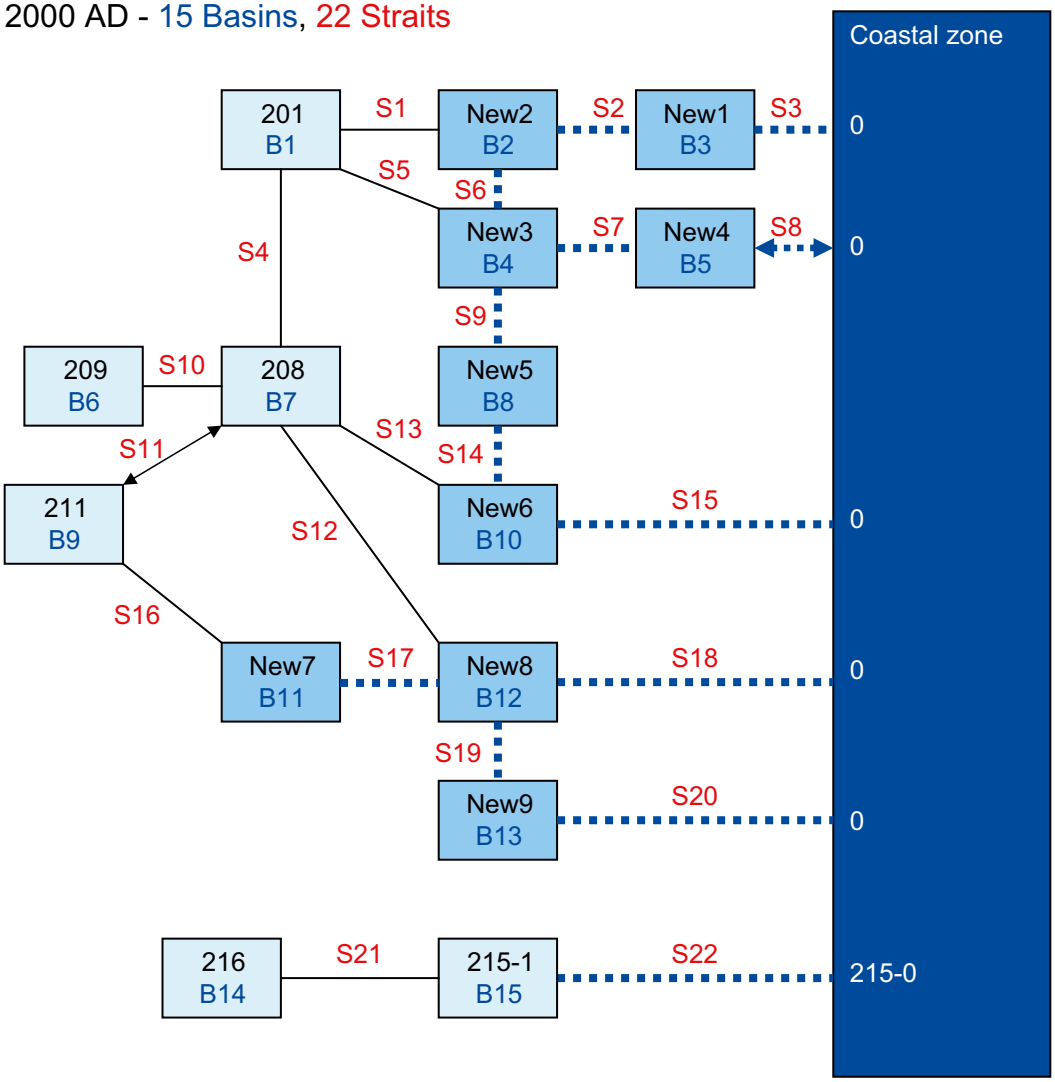

Figure A-6b. *Resulting coupled discrete basin configuration with the interconnecting straits enumerated in systematic order. The straits that do not coincide with biosphere basin interfaces are marked with broken blue lines. The necessity of introducing nine additional new SBs is a consequence of the increased complexity of the coast line as the land rises. The straits S8 and S11 were entered into the modeled configuration but they were later found to be blocked as their sill heights were higher than the peak of the sea level forcing. Since alternate pathways of water exchange exist, the SBs connected by these straits remain in active exchange with the open CZ.*

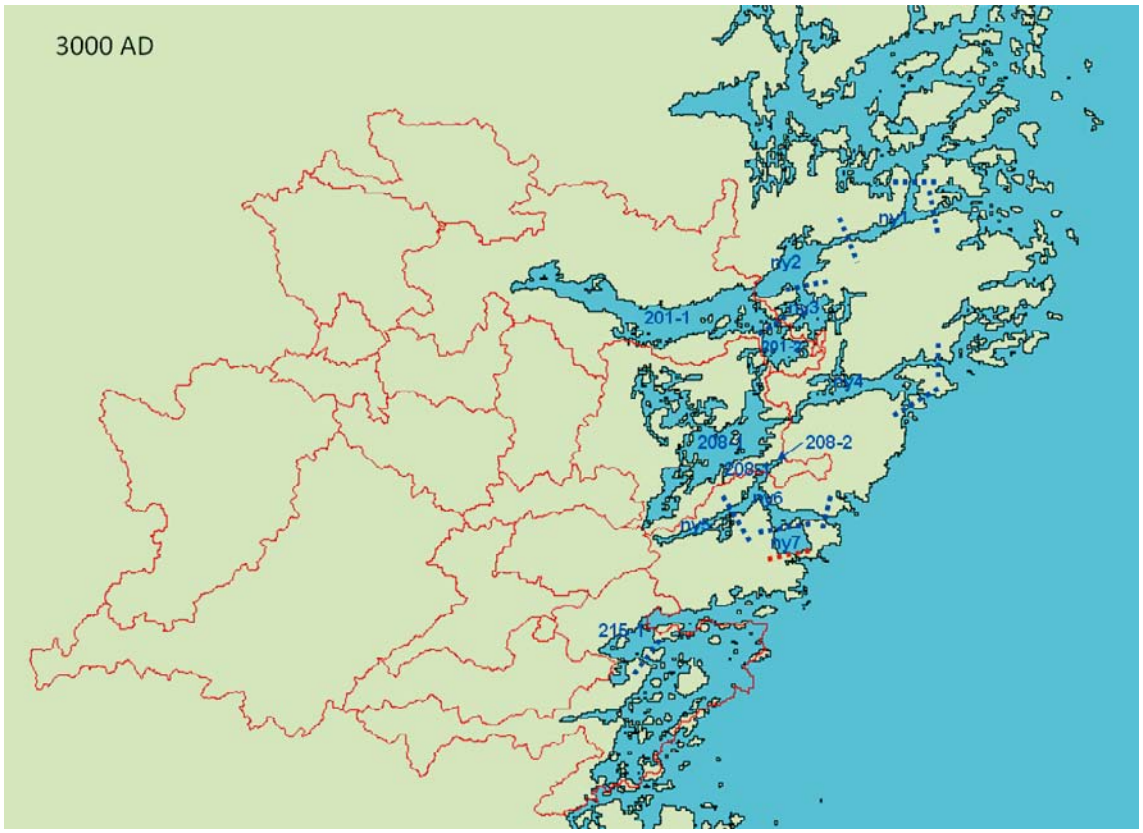

Figure A-7a. *Delimitation of the coastal basins with the shoreline of the year 3000 AD. Seven new basins needed to be added. The straits that do not coincide with biosphere basin interfaces are marked with broken blue lines. As the land progressively rises, several new extra SBs are needed towards the CZ in order to make the water exchange realistic. For graphical reasons these additional SBs have been indicated with with 'ny' instead of 'new'. As for Figure A6a, the southern occurring embayment of BO 215 has been omitted from the model computations since it is not associated with any exit points.*

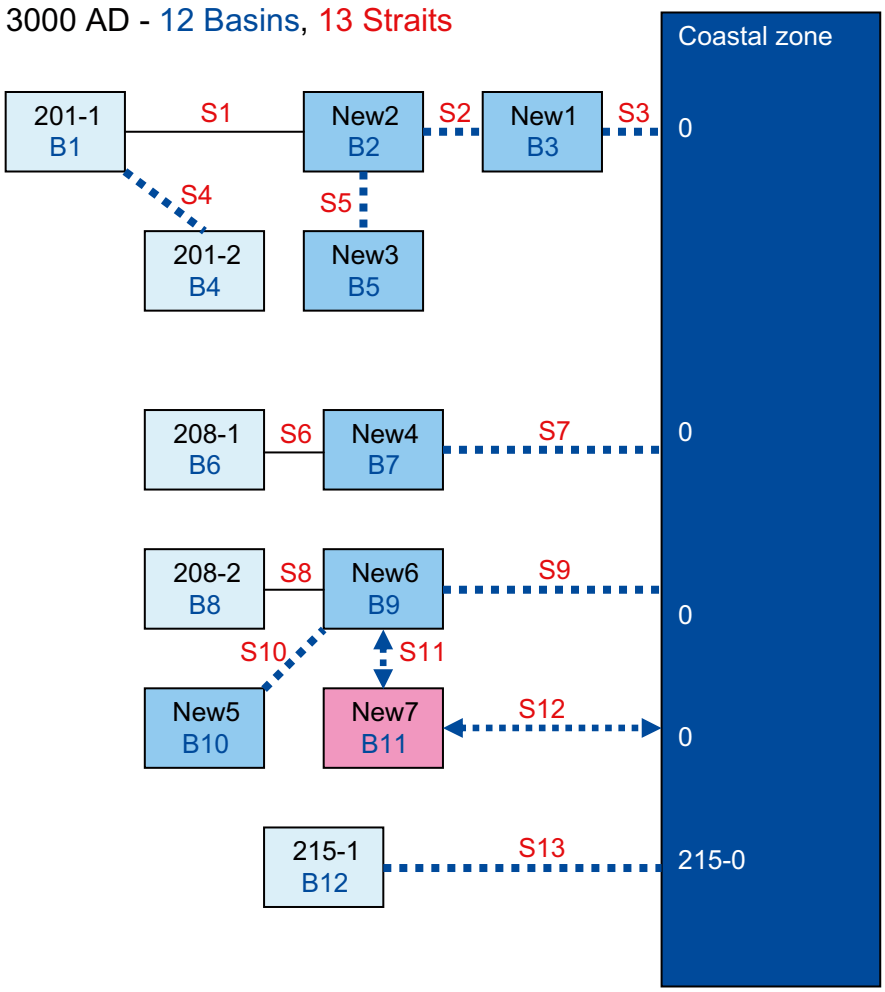

Figure A-7b. *Resulting coupled discrete basin configuration with the interconnecting straits enumerated in systematic order. The straits that do not coincide with biosphere basin interfaces are marked with broken blue lines. Only one internal circulation loop occurs (S9-S11-S12) but in this loop the sill heights of both S11 and S12 were found to exceed the peak of the sea level and thus the SB New7 could have been excluded from being subjected to the model. This involves a methodological problem which is discussed in Chapter 6.*

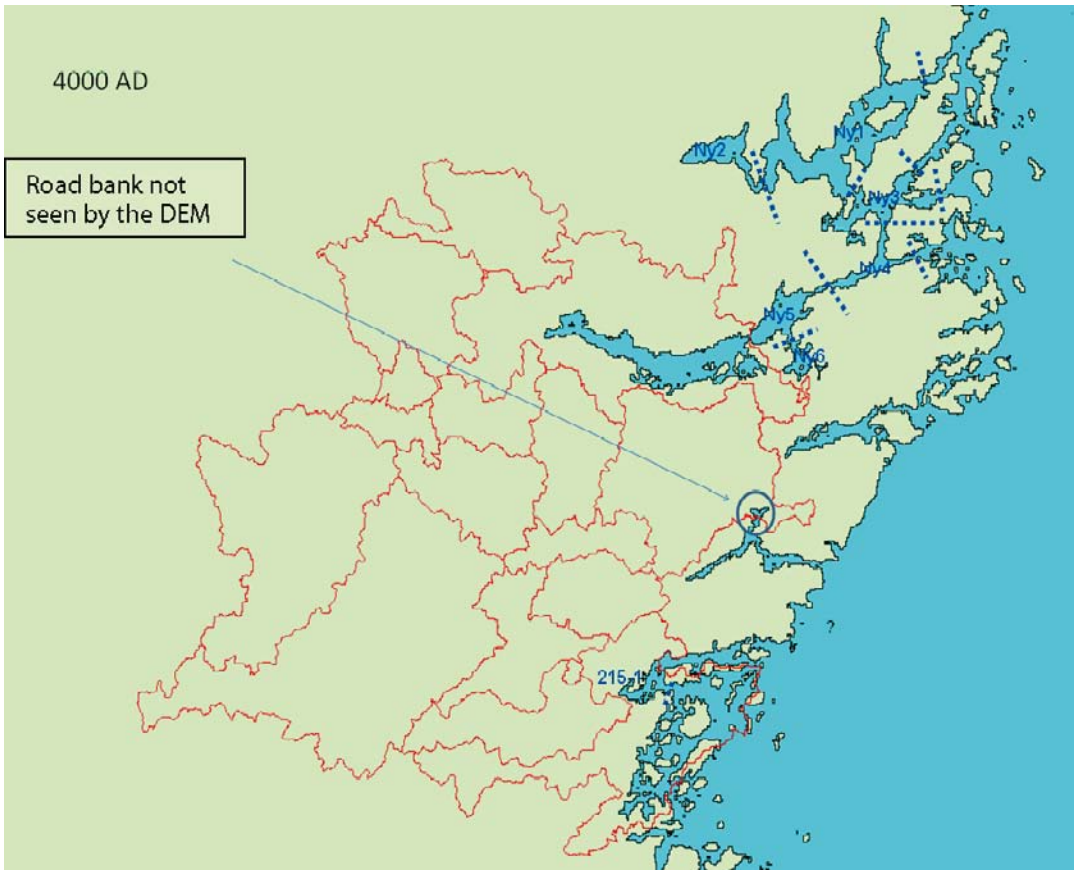

Figure A-8a. *Delimitation of the coastal basins with the shoreline of the year 4000 AD. The straits that do not coincide with biosphere basin interfaces are marked with broken blue lines. As the land rises seven new extra SBs are needed towards the open coast in order to make the water exchange realistic. For graphical reasons these additional SBs have been indicated with with 'ny' instead of 'new'. As for Figure A-6a, the southern occurring embayment of BO 215 has been omitted from the model computations since it is not associated with any exit points.*

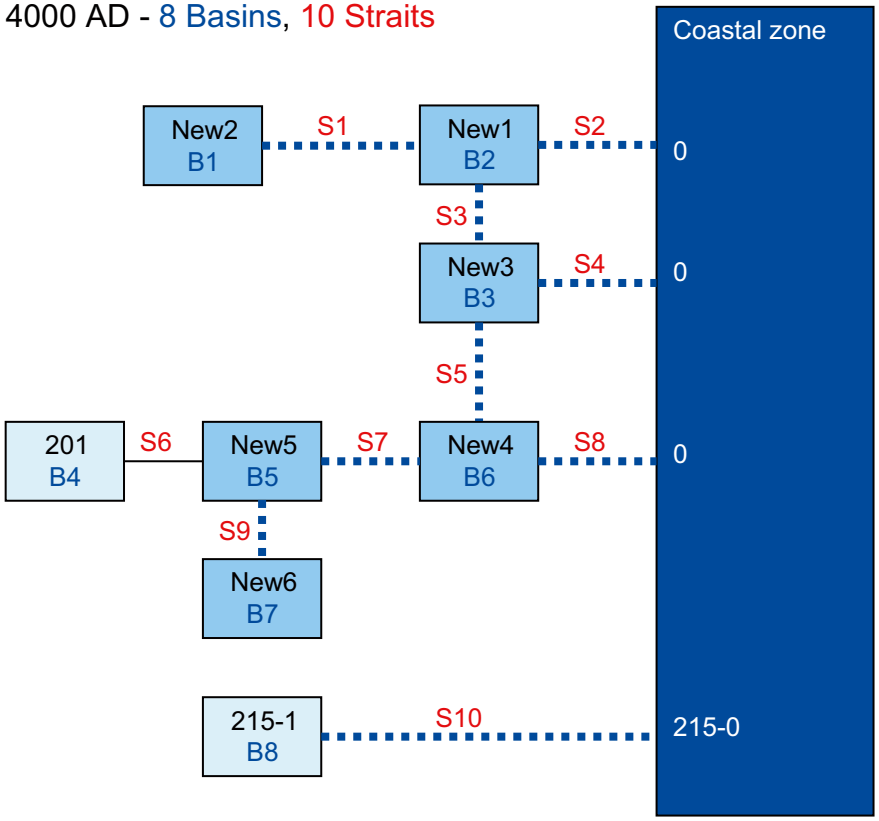

Figure A-8b. *Resulting coupled discrete basin configuration with the interconnecting straits enumerated in systematic order. The straits that do not coincide with BO-interfaces are marked with broken blue lines. Seven new basins are necessitated and it is evident that these outnumber the BOs. Two new internal circulation loops occur (S2-S3-S4) and (S4-S5-S8).*

Figure A-9a. *Delimitation of the coastal basins with the shoreline of the year 5000 AD. Five new basins needed to be added. The straits that do not coincide with biosphere basin interfaces are marked with broken blue lines. For graphical space reasons these additional sub-basins have been indicated with with 'ny' instead of 'new'.*

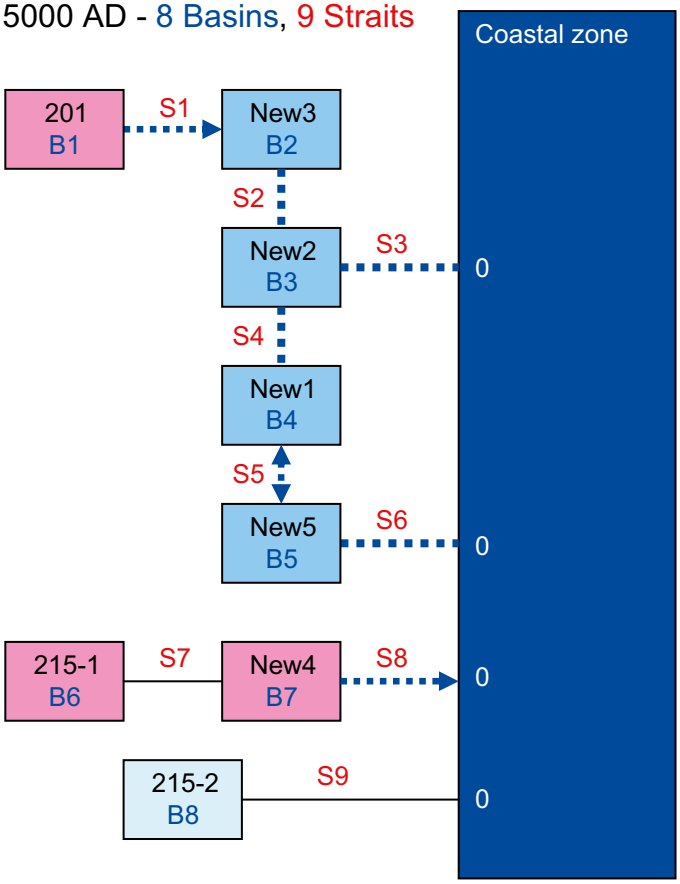

Figure A-9b. *Resulting coupled discrete basin configuration with the interconnecting straits enumerated in systematic order. The straits that do not coincide with biosphere basin interfaces are marked with broken blue lines. Five new basins are initially necessitated to make the connection to the open coast realistic. One of these (New4) is disconnected from the coastal zone by the shallow strait S8 with a higher sill level than the peak of the sea level forcing. The internal circulation loop (S3-S4-S5-S6) is interrupted by S5 that turned out to be shallower than the maximum of the sea level forcing.*

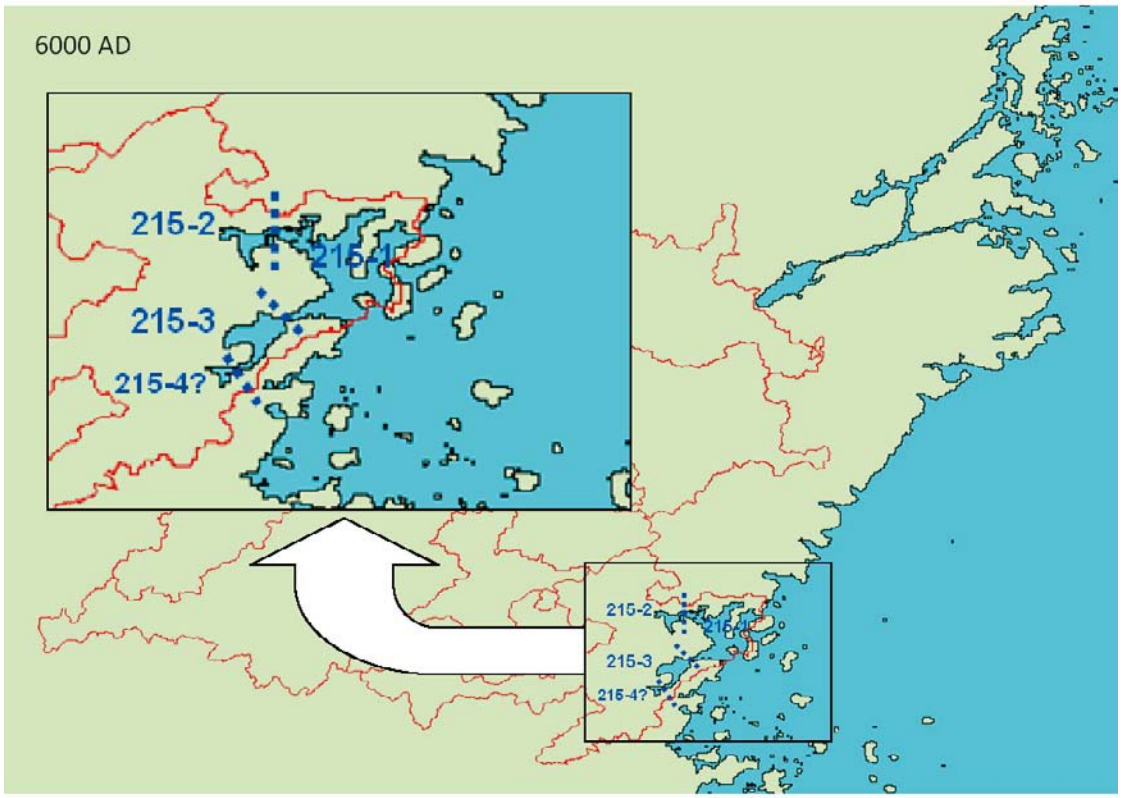

Figure A-10a. *Delimitation of the coastal basins with the shoreline of the year 6000 AD. These are confined to the southern part of the Laxemar/Simpevarp area and are shown as an inset enlarged map. No new basins are needed to complement the connection with the open coast. The relevant biosphere object basin consists entirely of BO 215,that was partitioned into four SBs, shown in the inset magnification. One single strait coincides with the biosphere basin interface; the others are marked with broken blue lines.*

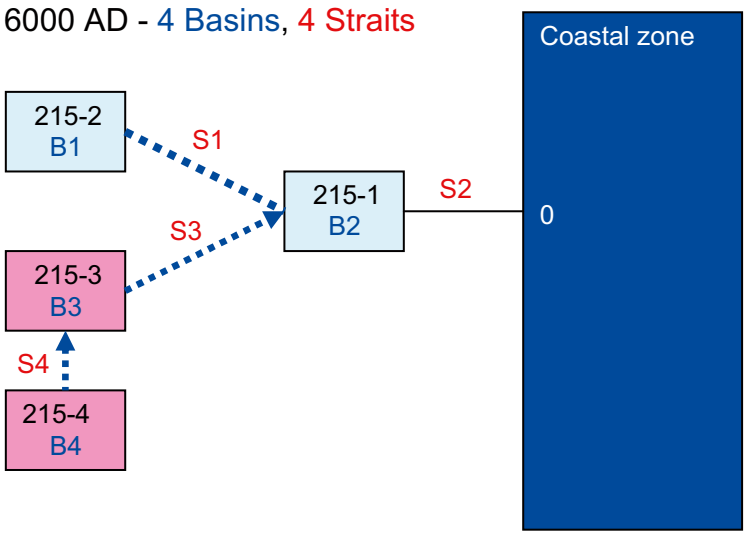

Figure A-10b. *Resulting coupled discrete basin configuration with the interconnecting straits enumerated in systematic order. The straits that do not coincide with biosphere basin interfaces are marked with broken blue lines. In retrospect two of the straits (S3 and S4) were found to be shallower than the peak of the sea level maximum, leaving effectively only B1 and B2 to be in active exchange with the coastal zone. The collective discharge of SBs 215-3 and 215-4 will act to increase the AvA-value of the other two SBs (215-1 and 215-2) of the same BO 215 of which they are a part.*

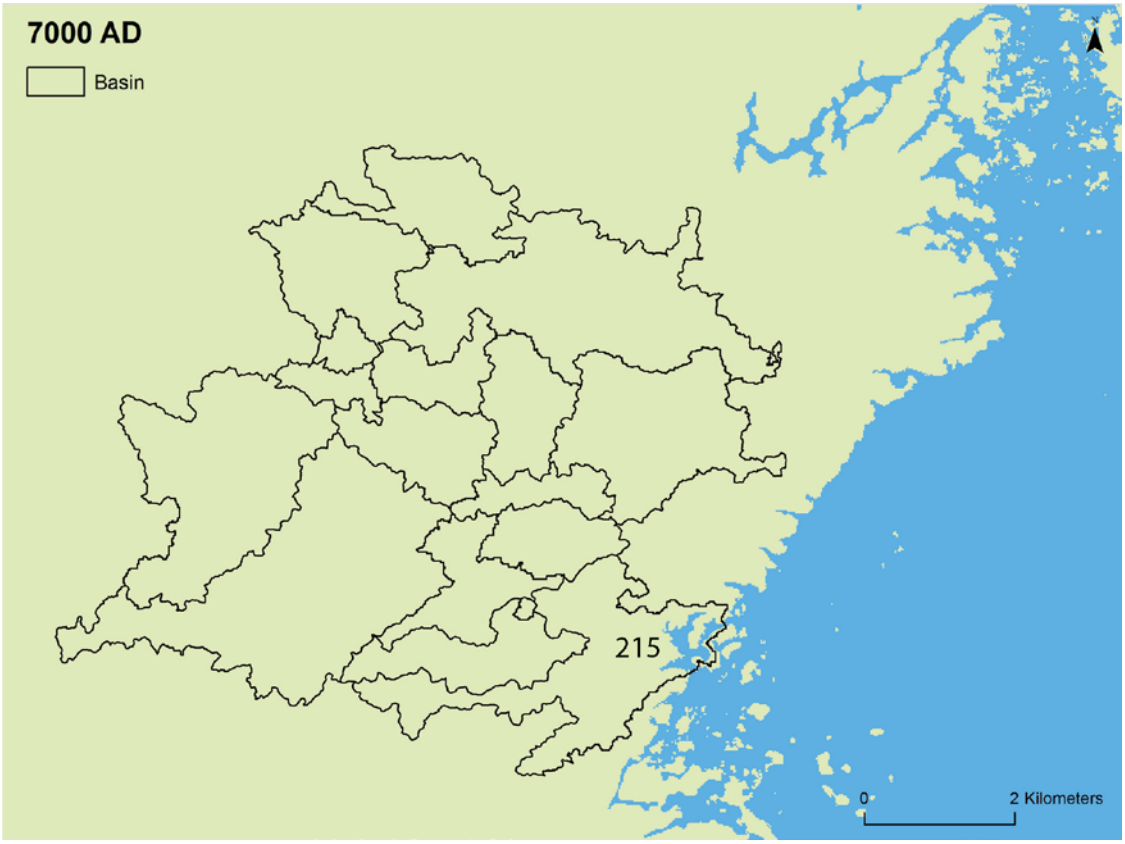

Figure A-11a. *Delimitation of the coastal basins with the shoreline of the year 7000 AD. The coastal embayment is reduced to one single BO, namely 215, which connects to the CZ by a single, however wide, strait coinciding with the silled interface.*

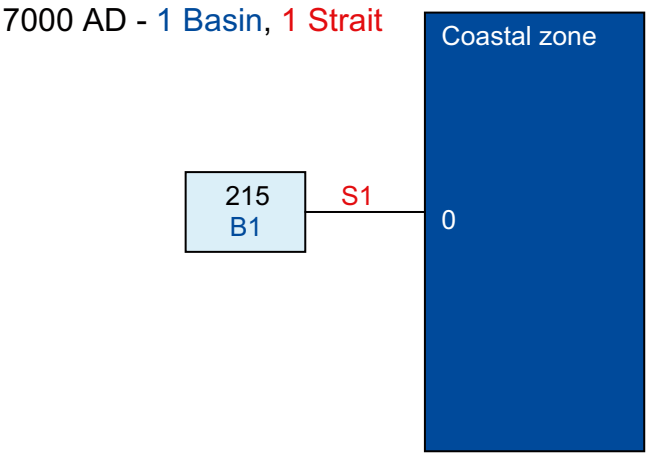

Figure A-11b. *Resulting coupled discrete basin configuration with the interconnecting straits enumerated in systematic order. This represents the simplest possible configuration.*

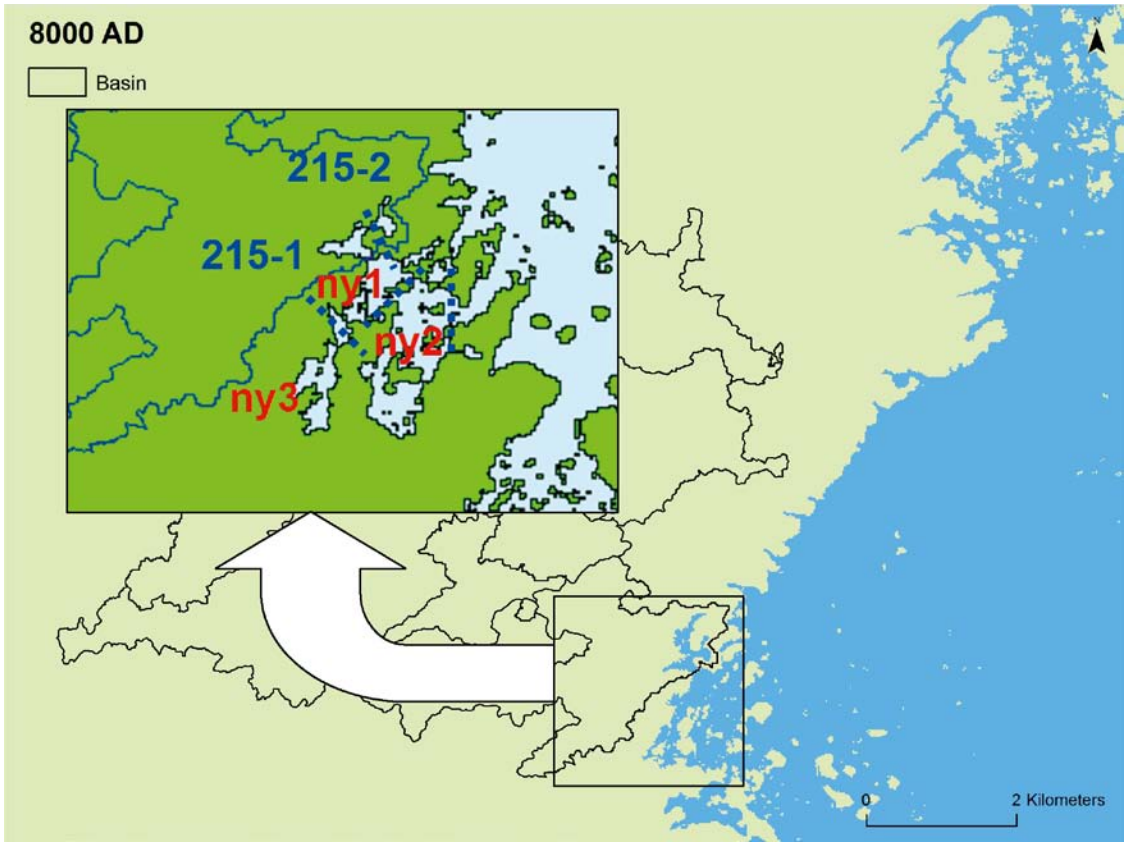

Figure A-12a. *Delimitation of the coastal basins with the shoreline of the year 8000 AD. The active SBs are still confined to the southern part of the Laxemar-Simpevarp area and are shown in the inset enlarged map. Three new basins are needed to complement the connection with the open coast. The relevant BO consists entirely of 215, that was partitioned into two sub-basins.*

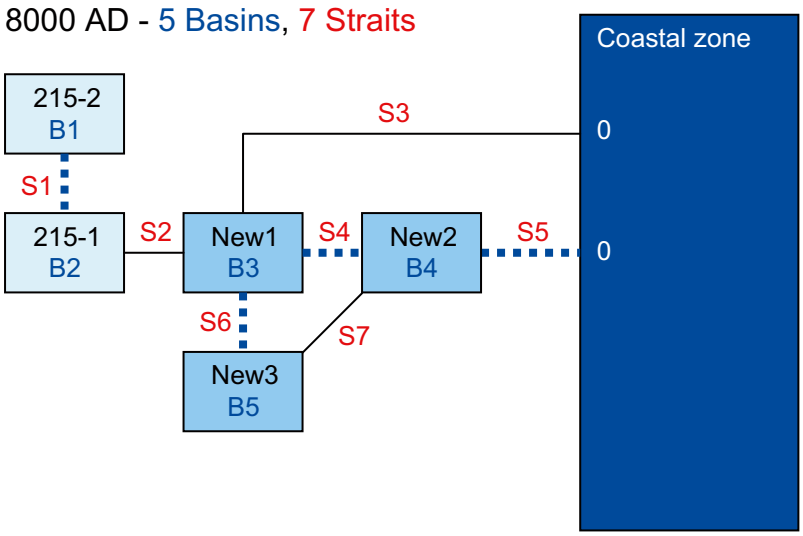

Figure A-12b. *Resulting coupled discrete basin configuration with the interconnecting straits enumerated in systematic order. The straits that do not coincide with BO-interfaces are marked with broken blue lines. Two internal circulation loops occur as the receding shoreline converts more underwater structures to become straits.*

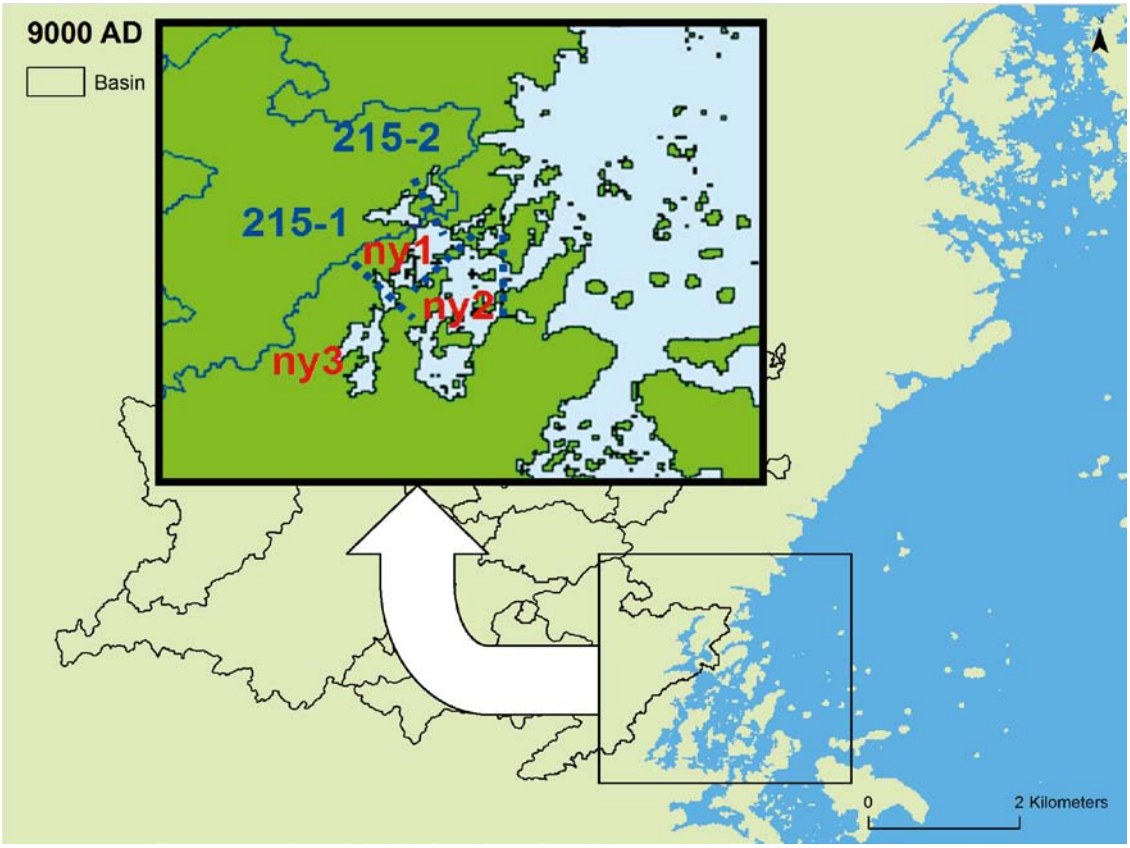

Figure A-13a. *Delimitation of the coastal basins with the shoreline of the year 9000 AD. The active SBs are still confined to the southern part of the Laxemar/Simpevarp area and are shown in the inset enlarged map. Three new basins are needed to complement the connection with the open coast. The relevant BO consists entirely of 215 that needed to be partitioned into two SBs.*

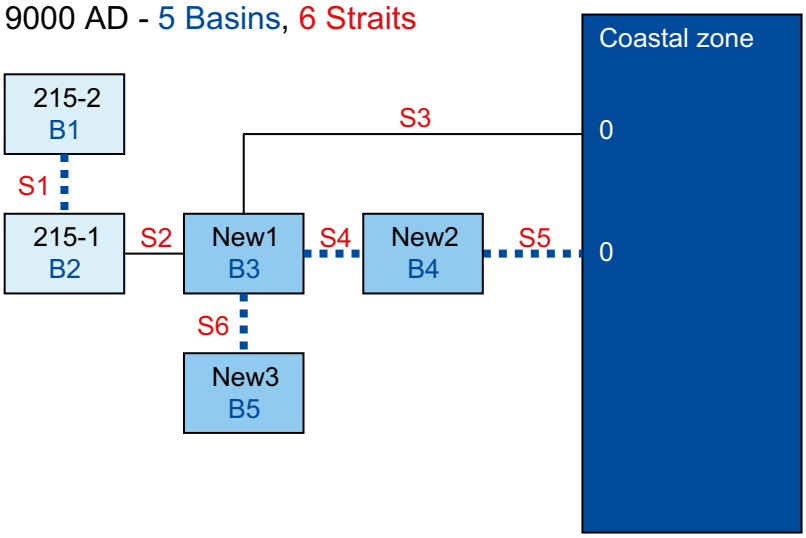

Figure A-13b. *Resulting coupled discrete basin configuration with the interconnecting straits enumerated in systematic order. The basin configuration is mainly the same as for 8000 AD (Figure A12b) with the exception of the strait S7 that no longer exists. Note that even though the labeling of the new SBs is the same as for 1,000 years earlier, the corresponding basins have evolved and do not denote the same physical basins.*

Appendix B

Resulting *AvA*-diagrams from the CouBa-model computations

In this appendix the following three abbreviations occur frequently: SB for sub-basin, BO for biosphere object and CZ for the coastal zone. The three-letter literal trailing the time period (e.g. '2cA' after 3000 BC) in the title of all 13 comprised diagrams denotes an ID-label to tell the different computer runs apart.

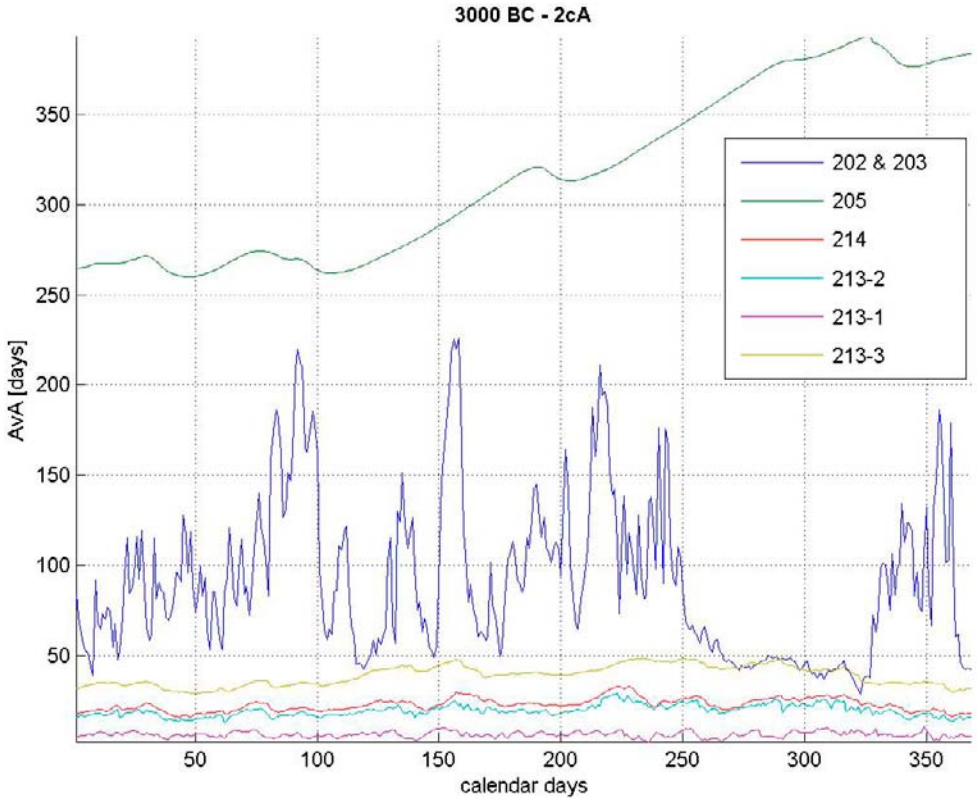

Figure B-1. *Graphical rendering of the AvA-computation for 3000 BC. With the exception of BO 205 all other SBs reach quasi-stationary AvA-levels. The seasonal variance is accentuated for the subsequently conjoined BO basins 202 and 203.*

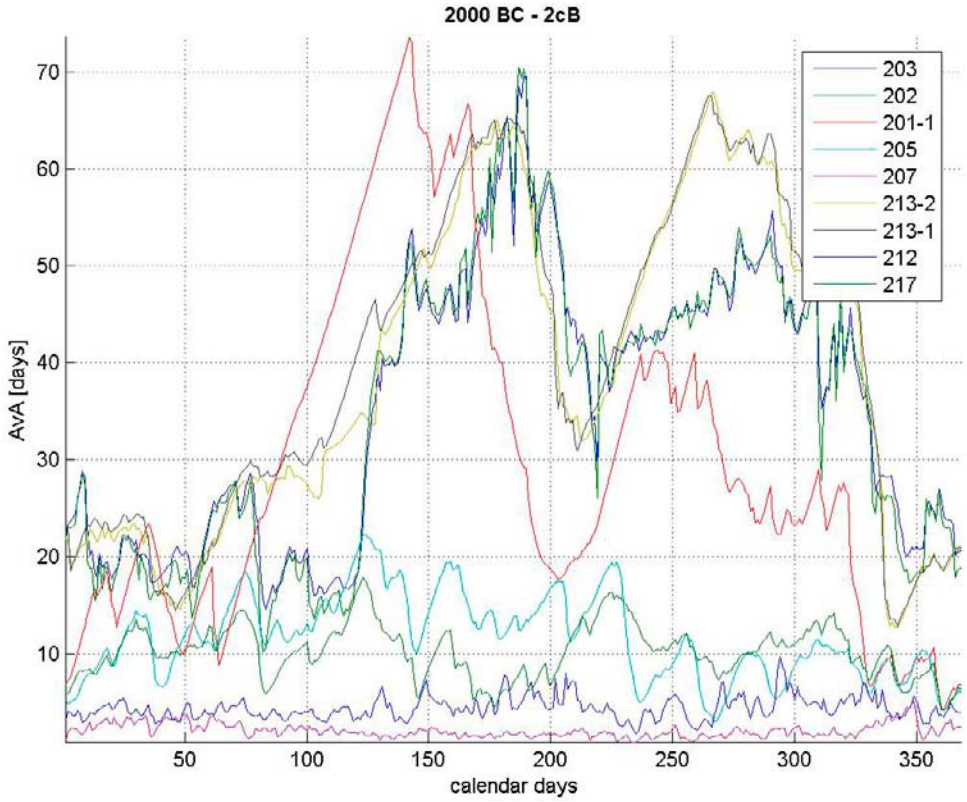

Figure B-2. *Graphical rendering of the AvA-computation for 2000 BC. All involved SBs attain quasi-stationary levels. The seasonal variance is accentuated for the subsequently conjoined basins of the BOs 202 and 203.*

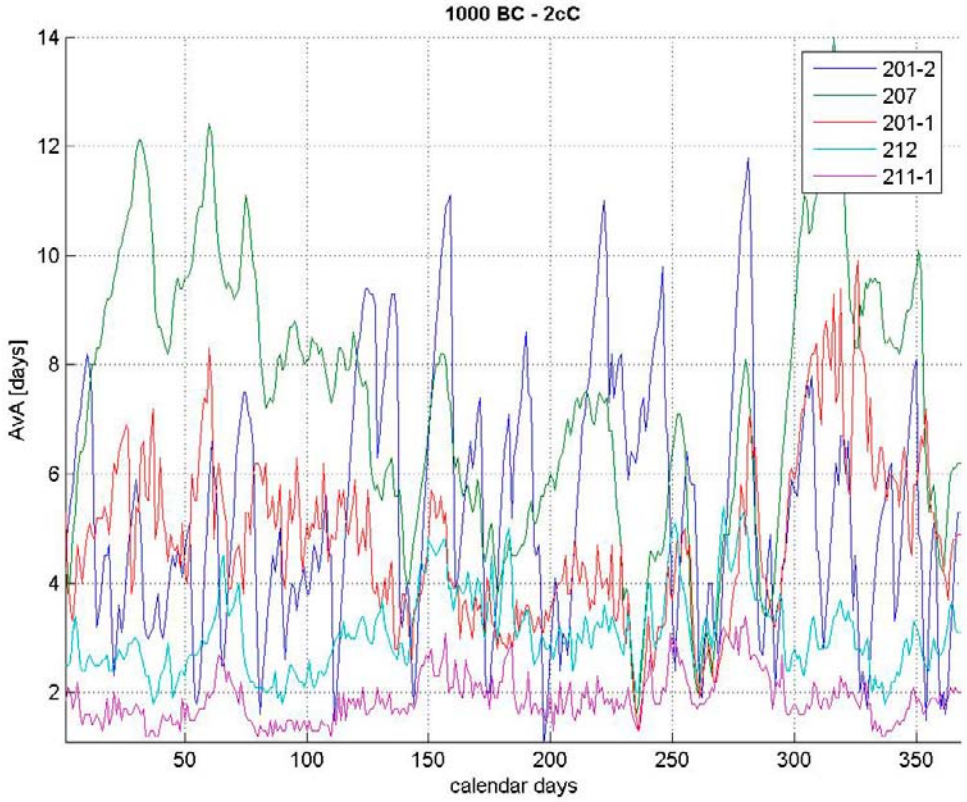

Figure B-3. *Graphical rendering of the AvA-computation for 1000 BC. All involved SBs attain stationary levels. The seasonal variance is generally quite conspicuous.*

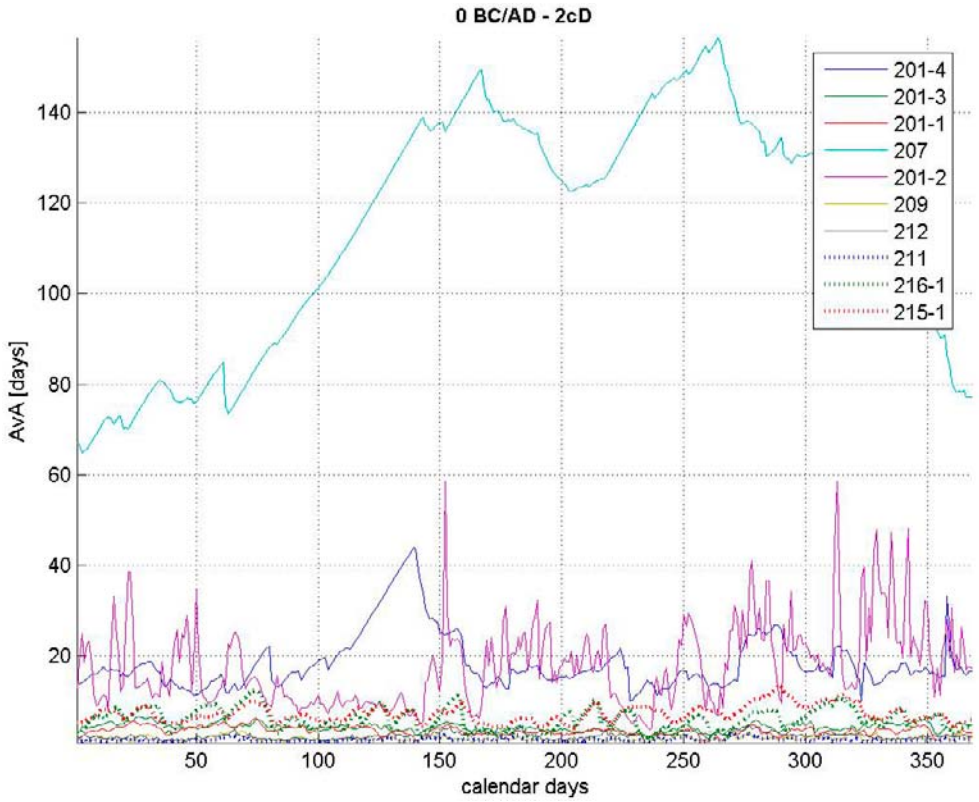

Figure B-4. *Graphical rendering of the AvA-computation for 0 AD/BC. All involved SBs, including BO 207, attain stationary levels. The seasonal variance is noticeable for all SBs.*

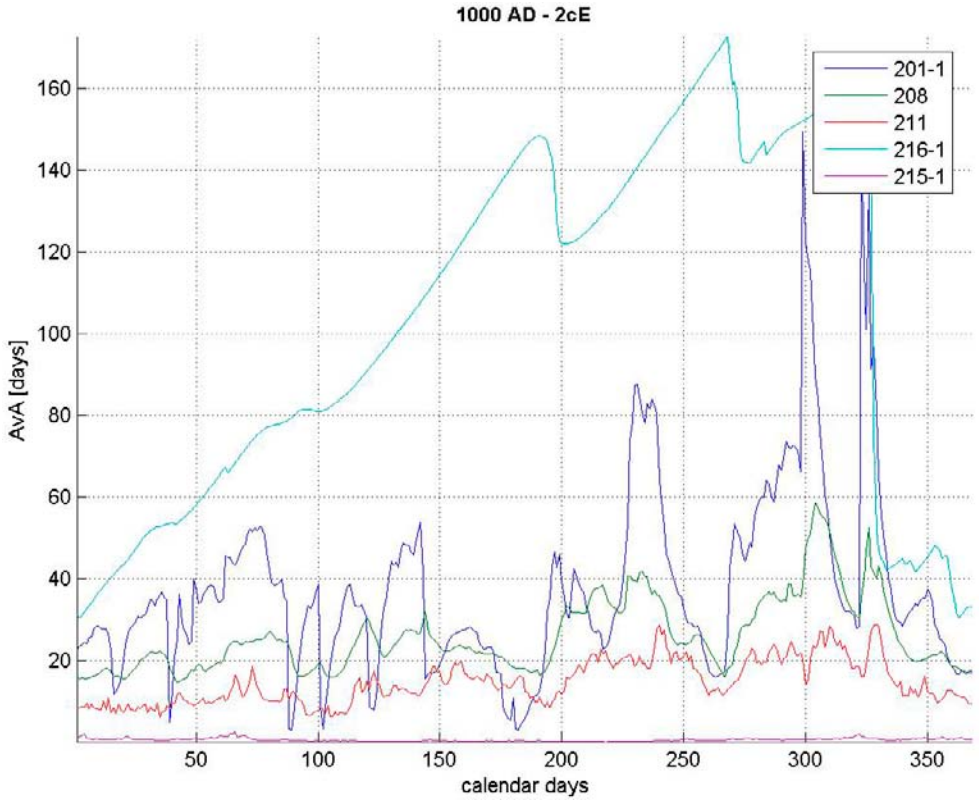

Figure B-5. *Graphical rendering of the AvA-computation for 1000 AD. All involved SBs attain quasi-stationary stationary AvA-levels. The seasonal variance is noticeable in particular for SB 216-1, while SB 215-1 could be considered as part of the CZ.*

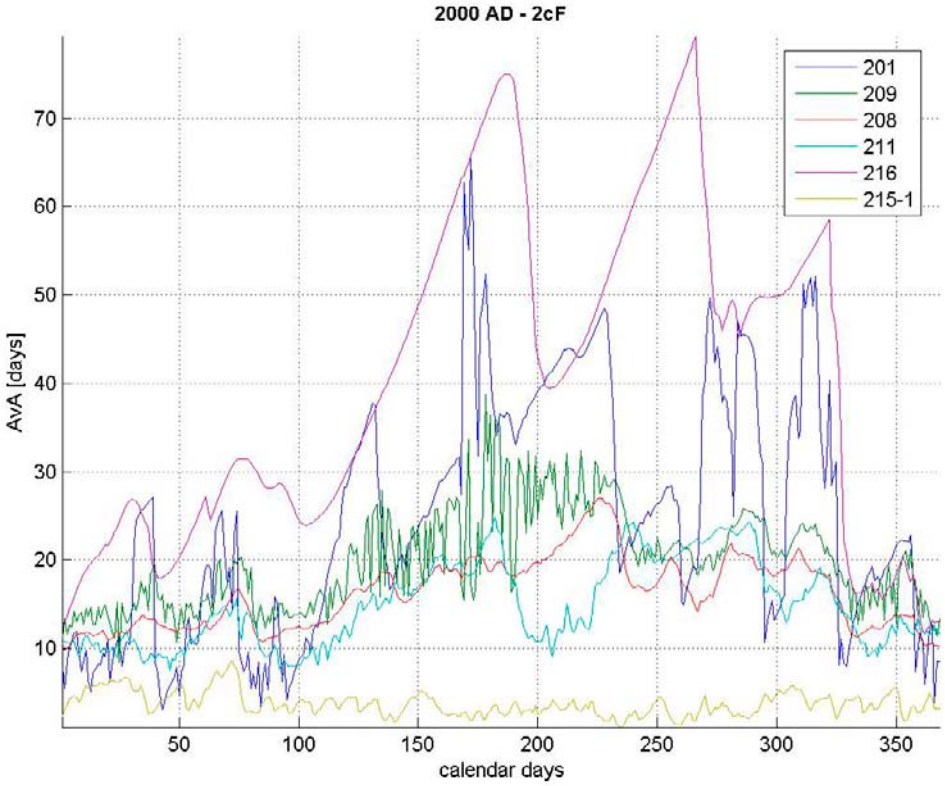

Figure B-6. *Graphical rendering of the AvA-computation for 2000 AD. All involved SBs attain quasi-stationary stationary AvA-levels. The seasonal variance is noticeable in particular for BO 216. The average of these AvA-levels can be compared to the results in /Engqvist 2006/, which comparison is expounded in Table 6-1 and Figure 6-1.*

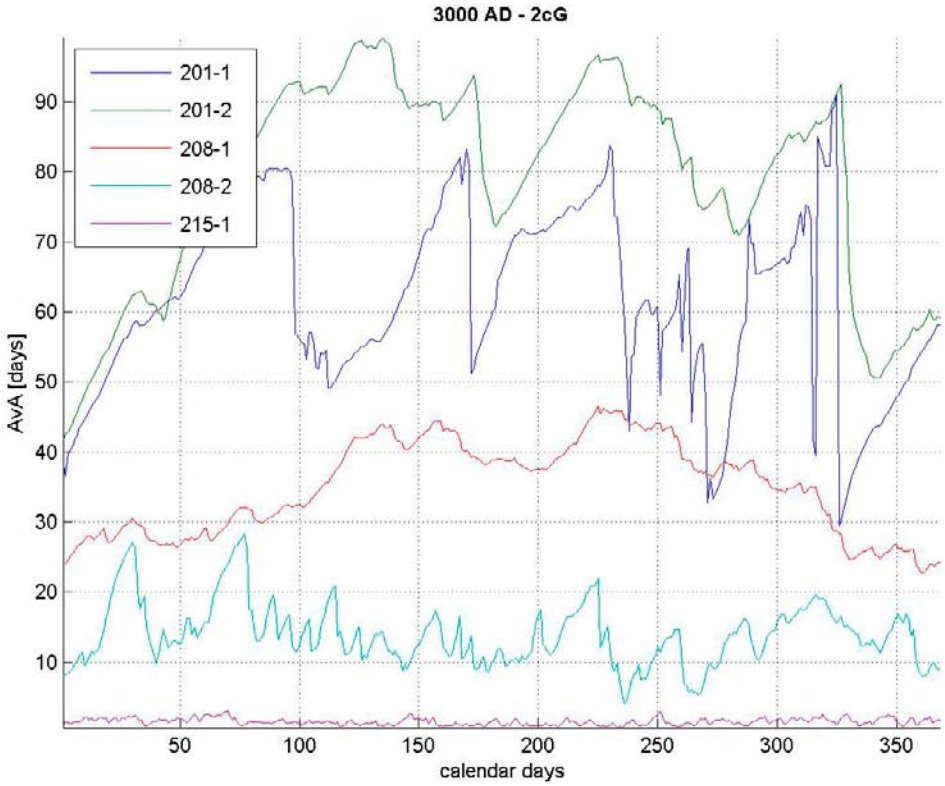

Figure B-7. *Graphical rendering of the AvA-computation for 3000 AD. All involved SBs attain quasi-stationary stationary AvA-levels. The seasonal variance is noticeable for most SBs. The comparatively low AvA-value of SB 215-1 makes it a candidate to be considered as belonging to the CZ.*

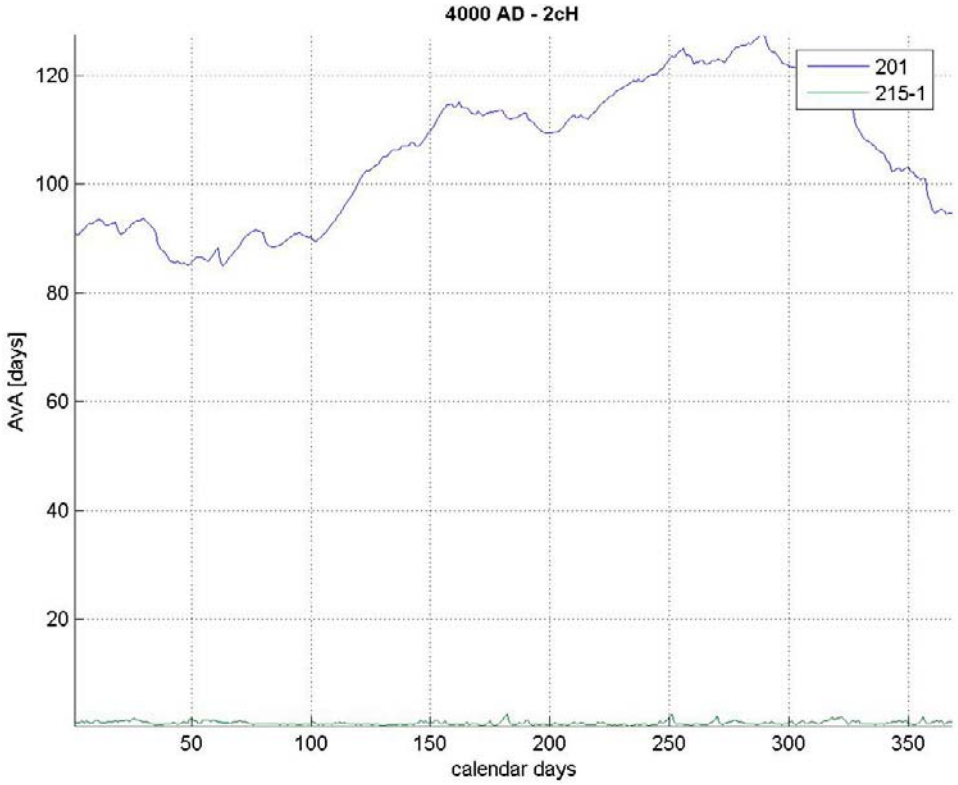

Figure B-8. *Graphical rendering of the AvA-computation for 4000 AD. Both SBs attain quasi-stationary stationary AvA-levels. The seasonal variance is more pronounced for the BO 201, while as for the previous time periods SB 215-1 is intense exchange with the CZ.*

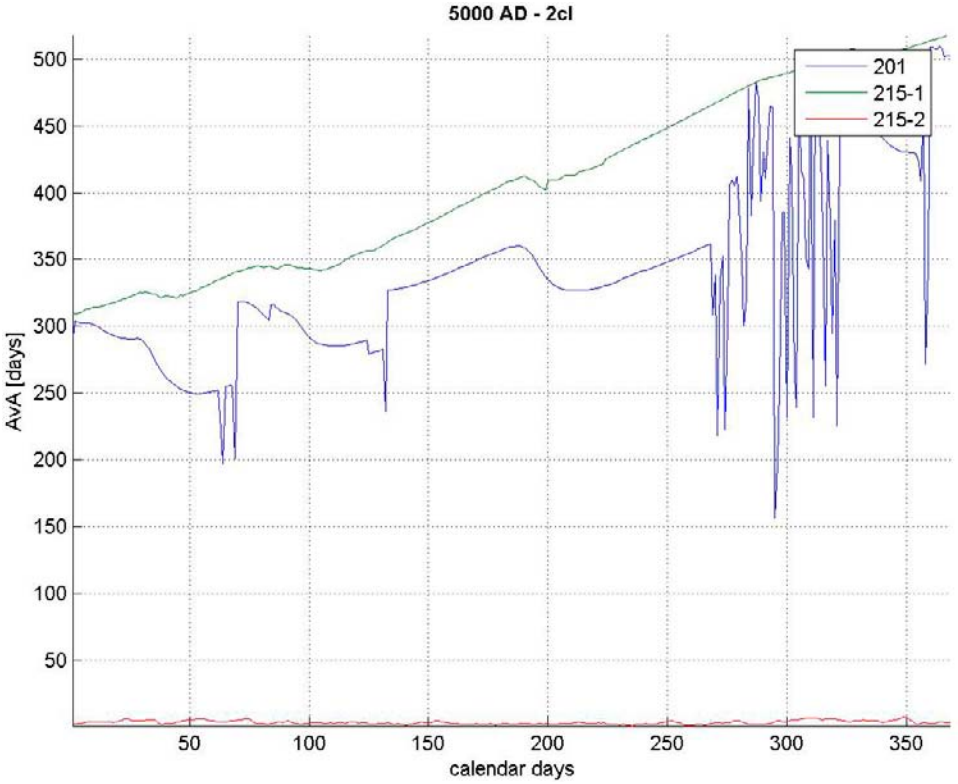

Figure B-9. *Graphical rendering of the AvA-computation for 5000 AD. Only the SB 215-2 attains a quasi-stationary stationary AvA-level. The other two SBs are thus not sufficiently hydraulically connected to the open coastal zone to be considered coastal embayments.*

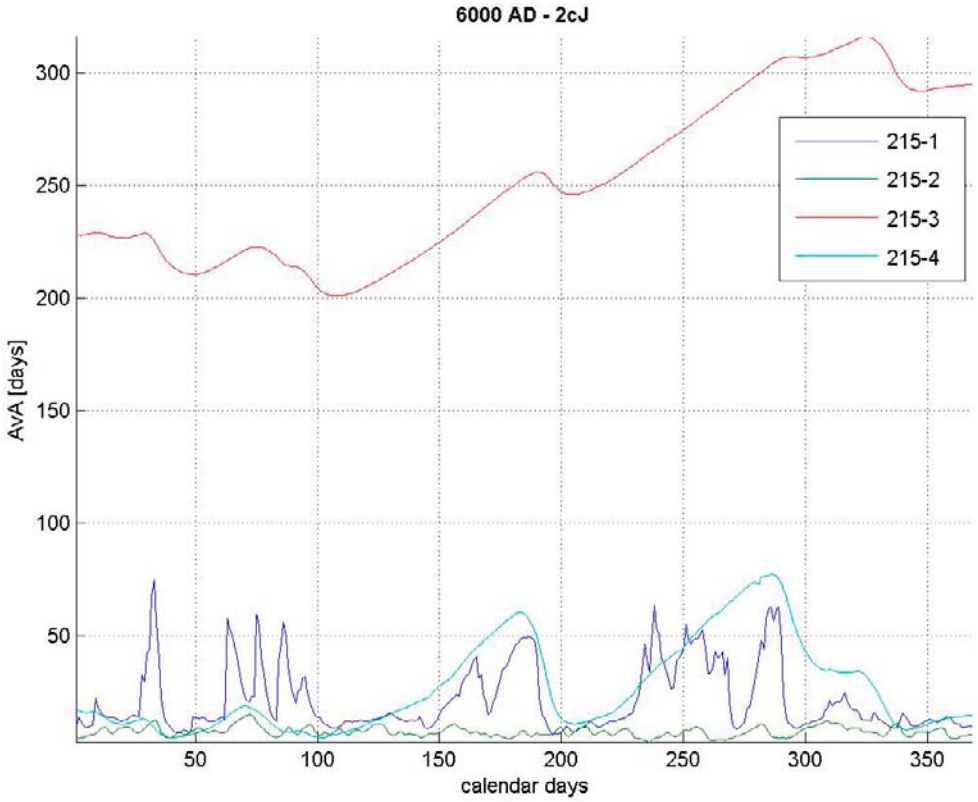

Figure B-10. *Graphical rendering of the AvA-computation for 6000 AD. Only the SB 215-2 does not attain a quasi-stationary AvA-level. The other three are sufficiently hydraulically connected to the open coastal zone to achieve a valid AvA-value.*

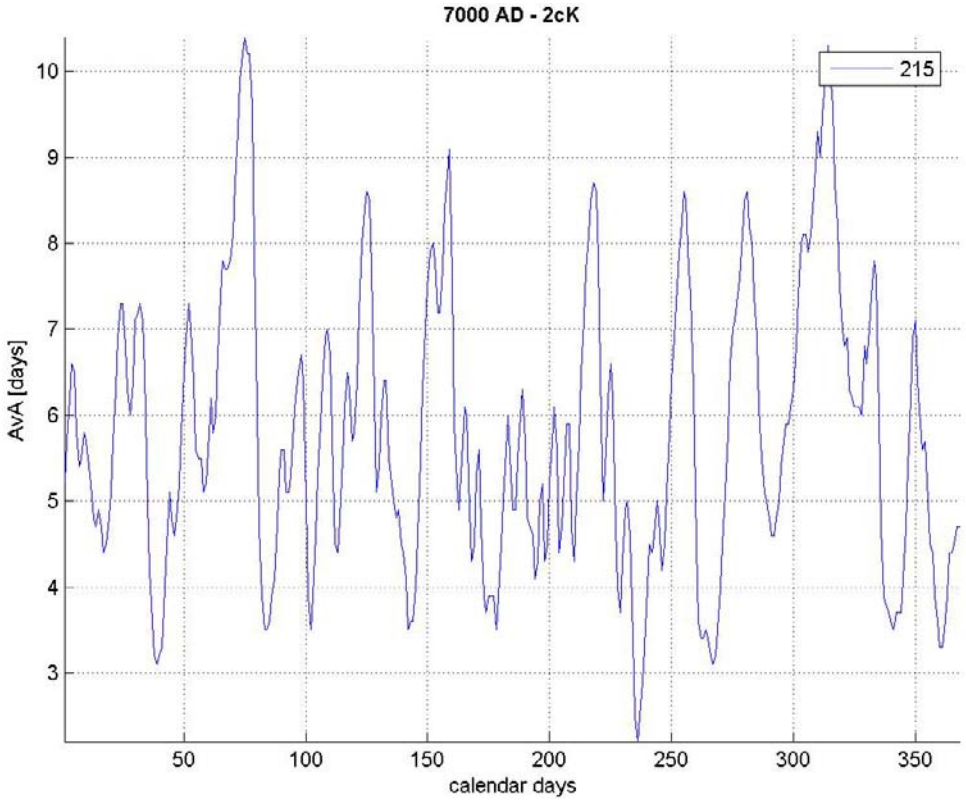

Figure B-11. *Graphical rendering of the AvA-computation for 7000 AD. The single SB coinciding with BO 215 certainly attains a quasi-stationary AvA-level with an accentuated seasonal variance.*

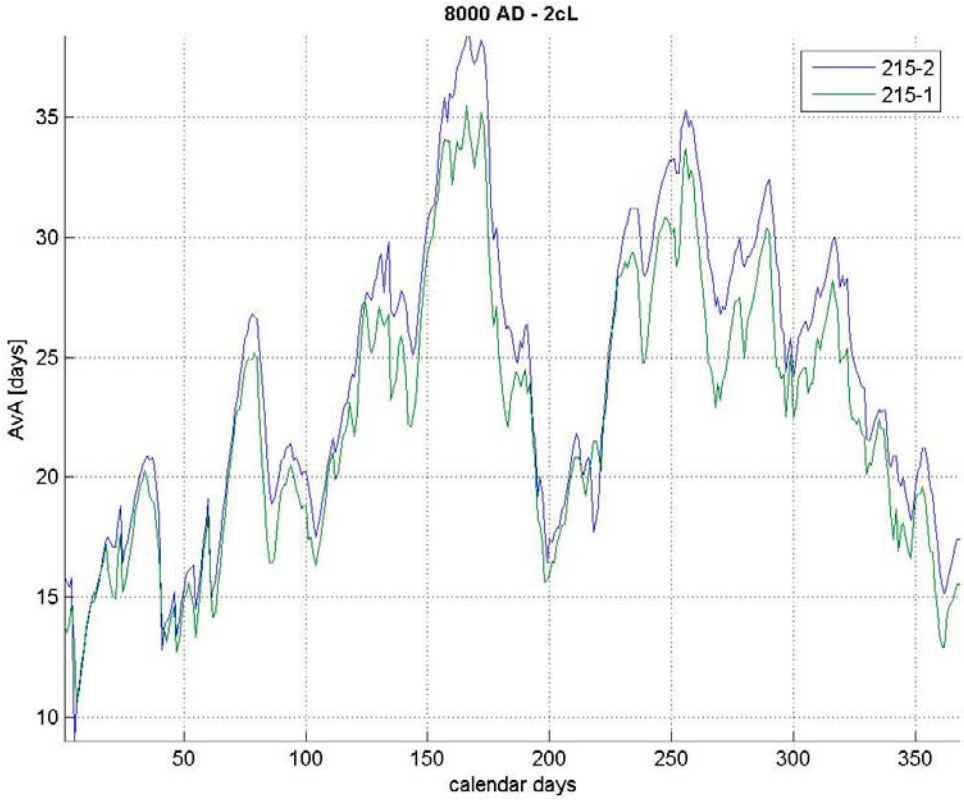

Figure B-12. *Graphical rendering of the AvA-computation for 6000 AD. Both SBs attain almost identical quasi-stationary AvA-levels with an evident degree of seasonal variance.*

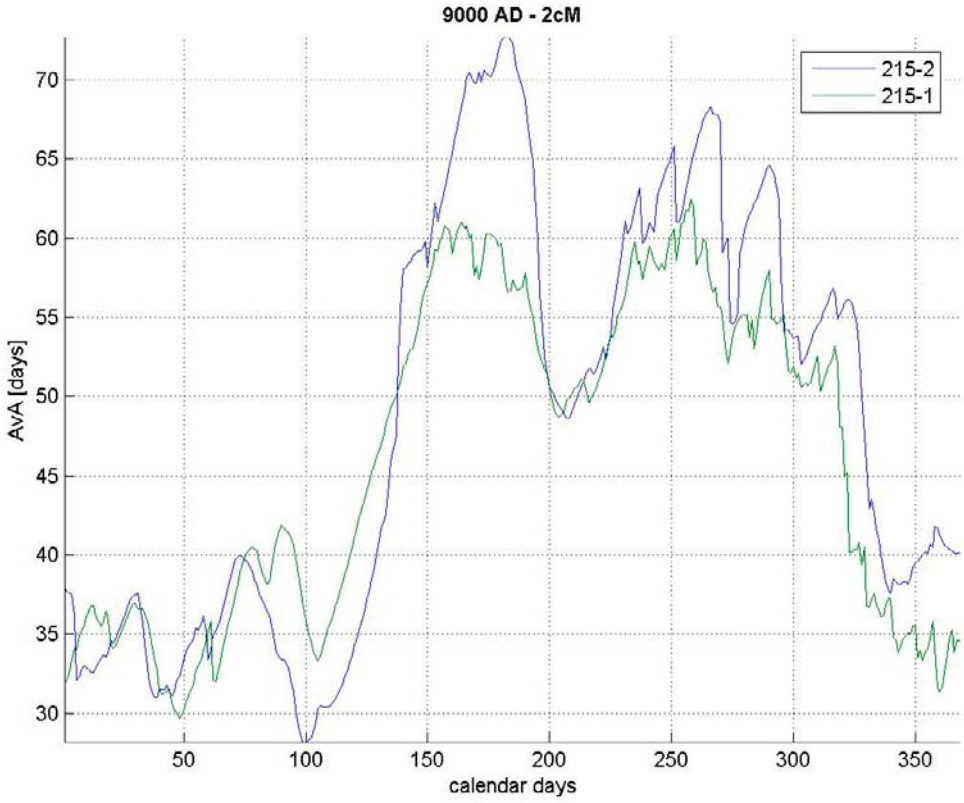

Figure B-13. *Graphical rendering of the AvA-computation for 6000 AD. Both SBs attain quasi-stationary AvA-levels with an evident degree of seasonal variance and covariance even though even though the similarity is not as striking as for 8000 AD.*